



A comparative review on the structural behaviour of GFRP rebars with conventional steel rebars in reinforced concrete columns

Anjali Kumari Pravin Kumar Pandey¹ · Mostafa Dada¹ · M. Longshithung Patton¹ · Dibyendu Adak¹

Received: 15 May 2024 / Accepted: 21 August 2024
© Springer Nature Switzerland AG 2024

Abstract

FRP reinforcement bars are advantageous in environments prone to corrosion, such as coastal areas, and in electromagnetically sensitive zones. They are an appealing alternative to steel-reinforced concrete structures, which require frequent maintenance. Despite their benefits, the behaviour of FRP-reinforced concrete columns is complex and less explored than their use in beams and slabs, limiting broader application. This paper aims to provide insights into the structural characteristics of concrete columns reinforced with Fiber Reinforced Polymer (FRP) rebars, specifically GFRP bars, as alternatives to steel bars. It examines the influence of parameters such as aspect ratio, concrete type and grade, slenderness ratio, and reinforcement percentage on the strength and ductility of GFRP RCC columns under axial and eccentric loads. Design equations and numerical methods for predicting load-carrying capacity are summarised. The literature review reveals that GFRP RCC columns have 80–100% of the strength of steel RCC columns under concentric loading and 60–103% under eccentric loading, with a higher ductility index than steel RCC columns by an average of 17.4%. For NSC and HSC columns, GFRP bars contribute about 50% of the axial load-carrying capacity compared to steel bars. From the literature review in predicting the design load-bearing capacity of GFRP-RCC columns, it has been found that using the modulus of elasticity to determine the contribution of FRP longitudinal bars and employing concrete compressive strength rather than axial strain in FRP longitudinal bars contribution, yields more accurate predictions.

Keywords RCC columns · FRP bars · Longitudinal reinforcement · Compressive strength · Ductility

Introduction

In the design of structural concrete columns, strength and ductility are crucial factors to be considered. According to Sheikh and Uzumeri [1], these considerations can be improved by adding longitudinal reinforcement bars around the concrete core's perimeter and fastening these bars with laterals like ties. Steel bars are one of the primary structural elements utilised as reinforcing material in concrete due to

their strong bond with concrete and superior tensile resistance. However, the steel rebars corrode due to inadequate or porous concrete cover, poor craftsmanship and harsh weather conditions, as investigated by the authors [2–4]. Due to the various problems associated with steel rebars, many researchers have attempted to replace them with Fiber Reinforced Polymer (FRP) rebars. FRP rebar (such as Glass FRP (GFRP), Carbon FRP (CFRP), and Basalt FRP (BFRP), refer to Fig. 1) are a type of high-performance material made by embedding continuous fibres in a resin matrix and has very good tensile strength, light weight, corrosion resistance, non-conductive, non-magnetic, and cost-effective when compared to that of its steel counterpart [5–9].

Due to these advantages of FRP rebars over steel rebars, FRP rebars have been used as reinforcement for a variety of concrete structures, including chemical and wastewater treatment plants, sea walls, under water structures, bridge decks, rehabilitation, retrofitting and strengthening of structures, “soft eye” tunnelling, construction of buildings with

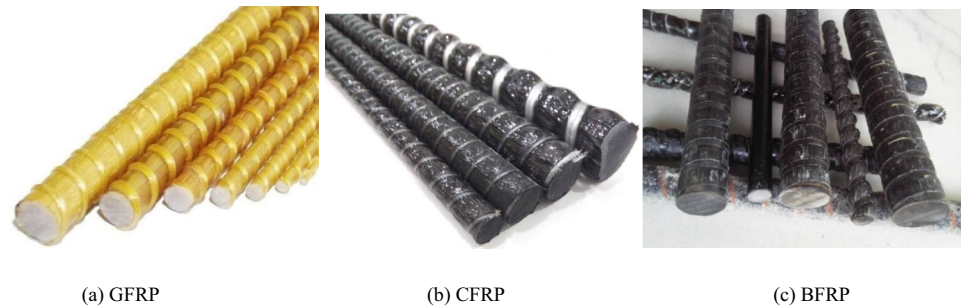
✉ Anjali Kumari Pravin Kumar Pandey
anjali.pandey.civil@gmail.com; ajkumari1996@gmail.com

Mostafa Dada
l.stivo.o@gmail.com

M. Longshithung Patton
nagaland22@gmail.com

Dibyendu Adak
dibu.ce@gmail.com; dadak@nitm.ac.in

¹ Department of Civil Engineering, National Institute of Technology Meghalaya, Shillong 793003, India

Fig. 1 Grooved FRP rebars

electromagnetically sensitive equipment and buildings in coastal areas [5, 9–16].

Despite the extensive research conducted on FRP as tubes and sheets over the past two decades [17, 18], investigations into utilising FRP rebars as structural frame elements have only commenced within the last decade, primarily focusing on beams, slabs, and some columns. Fan and Zhang [19] were among one of the earliest to conduct experiments on FRP-reinforced cement concrete (FRP-RCC) columns. Due to differences in their mechanical and physical properties, such as tensile strength, compressive strength, bond strength, and stress–strain behaviour, a direct substitution between FRP and steel rebar may not be a viable option. As a result, several researchers have conducted multiple experiments over the past few years to determine the behavioural similarities and differences between FRP-RCC columns and conventional steel-reinforced concrete (steel-RCC) columns. The present study conducts a descriptive literature review on the structural performance of FRP reinforcement bars in RCC columns. In addition, the study compares the benefits and drawbacks of FRP-RCC columns to those of conventionally used steel-RCC columns and provides conclusions and scope for future research in this area.

Significance of research

FRP reinforcement bars can be proven to have remarkable benefits in construction practices in coastal areas, electromagnetically sensitive regions, and industries sensitive to corrosion in structures, where steel-reinforced concrete structures prove to have less durability and frequent maintenance is required. However, as observed from the literature studies, FRP is resistant to corrosion and gives a higher tensile strength, but it is comparatively not as ductile as steel and has less bonding strength with concrete than steel. Although there is existing research on using FRP rebars as substitutes for steel rebars in reinforced concrete columns, the analysis and design of FRP reinforced concrete columns are complex due to factors such as bond strength, compressive strength, ductility, and others. The lack of comprehensive understanding of FRP rebar-reinforced concrete columns is a significant limitation to their widespread

application. Hence, it is crucial to comprehensively examine the structural properties of FRP-RCC columns. The authors of this review have compiled recent research on FRP rebar-reinforced concrete columns, with a primary focus on axial and eccentric loaded columns. This literature study's scope is limited to analysing the effect of substituting steel longitudinal bars with GFRP longitudinal bars on the structural performance of RCC columns. The aim is to provide valuable insights into the structural behaviour of these columns and the factors that affect them. The review also serves as a guide for future research in the study of FRP-RCC columns. The following points summarise the objectives of this literature review:

- Assessing the mechanical properties of FRP reinforcement bars in relation to steel reinforcement bars in terms of tensile strength, compressive strength, and bond strength with concrete.
- Comparing the studies conducted on the compressive strength and ductility of concrete columns reinforced with GFRP rebar versus steel rebar.
- Examining the impact of crucial parameters, such as the shape of the cross-section (circular, square, and rectangular), the type and grade of concrete, the slenderness ratio, and the ratios of longitudinal and transverse reinforcement, on the strength of GFRP-RCC columns compared to steel-RCC columns.
- Presenting a concise overview of the existing literature on design equations and computational methods used to predict the load-carrying capability of GFRP-RCC columns.
- Identifying potential areas for future research in analysing the structural behaviour of GFRP-RCC columns.

Mechanical behaviour of FRP rebars

General introduction

This section describes an overview of the research background on FRP rebars and compares the bond strength, critical tensile and compressive strengths of FRP rebars to that

of steel rebars, which will aid as a reference for subsequent analysis on the behaviour of FRP in RCC columns. Several authors [6–11, 14–16, 20, 21] have previously examined the mechanical behaviour of FRP rebars.

Bond strength of FRP rebars

Table 1, presented below, provides a compilation of some relevant scholarly works pertaining to the investigation of bond strength between FRP and conventional steel rebars and concrete. Figure 2 shows various bond mechanisms adopted in the study of bond strength for FRP and steel rebars.

It is observed from previous studies that without any surface treatment for ribless FRP rebar, steel rebar shows the highest bond strength followed by GFRP and the least in BFRP [22, 33] and also, the bond strength is governed by adhesion and friction [22]. However, FRPs with grooving or ribbed surfaces showed a bond strength which is at par with steel rebars [15, 25–27, 32]. From the studies, it was found that the bond strength of the grooved or ribbed FRPs can be further improved by the use of machine and sand-coated FRPs [20], the use of rebar-epoxy interface [23, 24, 26], and increasing the rib height [32]. Further, the bond strength of FRPs decreases with increasing diameters [22, 24]. Additionally, the bond between FRP and concrete significantly influences the failure mode, post-yield stiffness, residual displacement and ductility of the column. However, it does not substantially impact the column's elastic stiffness [25–27].

Tensile strength of FRP rebars

In addition to bond strength, FRP rebars' tensile and compressive strengths are crucial mechanical properties to consider when designing FRP-reinforced concrete columns. The characteristics of the current FRP systems vary substantially depending on their unique formulation, parts, and manufacturing process and are direction-sensitive [15, 20]. The properties of FRP composite materials are typically discovered by experimental testing of the FRP material and products. Generally, FRP rebars for structural engineering applications are made of glass, carbon, basalt, and aramid fibres since they have higher tensile strength than traditional steel.

Figure 3 illustrates that linear elastic tensile stress–strain behaviour is present in all FRP systems (in the direction of the fibres) and that FRP systems do not yield. Abbood et al. [8] discussed the mechanical properties of FRP composite materials in terms of compressive, shear, flexural, and tensile strength against extreme loading and environmental conditions and also reported that GFRP is the cheapest composite among other FRP materials. Figure 4 shows a typical failure of an FRP material under tension. Conventional steel rebar under tensile load fails by the development of necking

phenomena till rupture; however, FRP's rebar fails by successive brittle failures of the individual fibres until rupture of the whole FRP rebar occurs (see Fig. 4).

Table 2 highlights the tensile properties of steel and FRP rebar, representing the density (δ), modulus of elasticity (E_f) and tensile strength (f_t) from previous experimental studies [8, 15, 21, 34, 35]. It can be seen from Table 2 that, except for some CFRP rebar, FRP rebar has lower elastic moduli than steel. Moreover, the average increase in tensile strength of CFRP, BFRP, and GFRP rebars is six times, four times, and three times more than that of steel rebars, respectively.

Compressive strength of FRP rebars

Conventional steel rebars show almost identical tensile and compressive properties; however, in the case of FRPs, studies showed that the tensile and compressive properties are quite different. As such, it becomes imperative to ascertain the proportion of compressive strength and tensile strength for FRP bars, particularly concerning investigating the compressive strength of RCC columns. Table 3 cites some of the research done on FRP rebars' compressive strength, specifically on GFRP rebars. In Table 3, the average value of compressive strength (f_c), tensile strength (f_t), compressive elastic modulus (E_c) and tensile elastic modulus (E_t) is taken for a given diameter of rebars.

The data presented in Table 3 indicates that while the compressive and tensile elastic modulus of GFRP rebars remains relatively constant, the compressive strength of these rebars is approximately 70% of the tensile strength. One contributing factor to the reduced compressive strength in polymers is their tendency to undergo deformation and buckling when exposed to compressive loads. This can result in either individual crushing or a combination of crushing and buckling, ultimately leading to premature failure [37] (refer to Fig. 5). In the process of tensile loading, the fibres experience an effective force that causes them to be pulled in the direction of their length, thereby utilising their complete strength capacity [36] (refer to Fig. 4). During compression, the fibres undergo transverse stresses, which can result in the separation or weakening of the bond between the fibres and the matrix. Consequently, this can lead to a reduction in the compressive strength of the material.

Several factors that have been found to influence compressive strength include the diameter of the bar, the slenderness ratio, and the method used for testing [36–40]. Previous studies have demonstrated that bars with smaller diameters exhibit greater efficacy in withstanding compressive loads when compared to bars with larger diameters [36–38, 40]. Also, it was observed that larger diameter GFRP bars necessitate a more significant load for failure compared to smaller diameter bars. This is attributed to the increased size of the larger bars, which results in the

Table 1 Summary of research on the bond strength of FRP rebars

Source	Rebar type	FRP's bond mechanism	Result
Tighiouart and Benmokrane [22]	Steel and GFRP	Rebar's on concrete	GFRP bars have lower bond strength than steel rebars. For GFRP rebars, Bond strength is governed by adhesion and friction. The average maximum bond strength decreases with increased diameter of bars (12.7–25.4 mm)
Sharaky et. al. [23]	NSM-CFRP	Rebar-epoxy interface	The tested specimens displayed various bonding patterns and mechanisms of failure, including: Failure of the bar-epoxy interface Epoxy failure with concrete cracking Failure of the concrete-epoxy interface
Sasmal et al. [24]	NSM-CFRP	Rebar-epoxy interface with varying rib diameter and spacing (refer Fig. 2b)	Above 0.8 times the diameter of CFRP bars, as rib spacing decreases, bond strength increases As the epoxy strength increases, there is a corresponding drop in bond strength, as ultimate failure takes place in concrete
Ibrahim et. al. [25]	BFRP	Rebars on concrete, texture of FRP bars, bar diameter and location	Longitudinal reinforcement employing BFRP bars had no impact on column elastic stiffness FRP-concrete bond affects column failure mode, post-yield stiffness, residual displacement, and ductility
Ibrahim, Fahmy, and Wu [26]	BFRP	Rebars on concrete, surface texture, adhesive material and bar diameter	Surface-treated FRP bars improve rebar-concrete bonding in columns
Ibrahim, Fahmy, and Wu [27]	BFRP	Rebar's on concrete and surface texture	The adhesive material properties of FRP bars play a crucial role in regulating the binding mechanism of reinforced concrete structures
Al-Mahmoud [20]	Steel and CFRP	Rebars on concrete and machined and sand-coated CFRP (refer to Fig. 2c)	Failure modes, lateral strength, post-yield stiffness ratio, and ductility at peak lateral strength and failure depend on FRP bars' bond parameters Both machined and sand-coated CFRP rebars have two times the bond strength of ribbed steel rebars At post-ultimate bond strength, the CFRP rebar's bond strength is either equal to or greater than that of ribbed steel rebar
Veljkovic et. al. [29]	GFRP	Bar external surface, concrete mechanical properties and concrete cover	Concrete shrinkage also influences the binding strength of CFRP rebars due to the additional strain The low splitting tendency and specific rib geometry of GFRP bars developed better bond behaviour in the case of eccentric tests Hence, ribbed GFRP bars demonstrated outstanding bonding performance even with a low concrete cover
Irshidat [30]	GFRP, CFRP	Rebar's on concrete, bar diameter, development length, and fibre type	The development length was shortened, and the bond strength increased significantly by adding 0.2% Carbon Nano Tubes (CNTs) The failure mode of the FRP-concrete bond was influenced by bar diameter but not by CNT content or embedded length

Table 1 (continued)

Source	Rebar type	FRP's bond mechanism	Result
Zhao et al. [28]	SFCB (refer Fig. 2c and d)	SFCB on concrete	The cross-sectional size and the surface treatment of the rebars are the parameters that affect the bond strength
Reichenbach [15]	Steel, GFRP, CFRP, and BFRP	Grooved FRP rebar's	The bond stiffness and strength of the grooved FRP rebars are at par with those of standard steel reinforcement
Taha and Alnahhal [31]	BFRP	Rebars in plain and steel FRP-RCC under oceanic environment and high temperature (35 and 60 °C)	Bond strength retentions of BFRP bars ranged from 54 to 86% over a 50-year service life, depending on the type of concrete (plain and SFRC), surrounding mean annual temperature (5–35 °C), and degree of moisture (dry, moist, and moisture saturated)
Shan et al. [32]	BFRP, GFRP	Rebar's on concrete, surface characteristics, steel fibre content in concrete	Bond strength can be increased by increasing the height of the surface rib of the FRP rebar Increasing the rib height from 0 to 0.76 mm results in a substantial bond strength enhancement, elevating it from less than 2.5–30 MPa
Kim and Wang [33]	Steel, GFRP and BFRP	Rebars on concrete, Surface roughness, percentage of steel fibres, silica fumes to cement content, and grade of concrete	Bond strength is the highest in steel, followed by GFRP, and the lowest is in BFRP Of the three types of reinforcement, the post-peak residual bond stress of steel is the least favourable

NSM-FRP near surface mounted FRP, SFCB steel FRP composite bar

release of higher energy during the failure process [37]. It is important to note that while GFRP bars possess lower compressive strength relative to their tensile strength, they nonetheless demonstrate advantageous mechanical characteristics (higher compressive and tensile strengths), including a high strength-to-weight ratio and corrosion resistance compared to steel bars with the same diameter. Consequently, these properties render GFRP bars suitable for diverse applications within construction and civil engineering fields. Hence, all subsequent discussions of the FRP-RCC column will be mainly based on GFRP rebar.

GFRP-RCC column

General introduction

In recent years, there has been significant progress in research on utilising FRP rebars to reinforce compression members in structural concrete. In regard to the experimental study, a substantial number of laboratory tests were conducted to assess the response of GFRP-RCC columns. An overview of the descriptive literature on the structural characteristics (compressive strength and ductility) of GFRP-RCC columns is provided in this section.

Compressive strength

Considering the utilisation of GFRP-RCC columns in various structural applications, several researchers have recently undertaken investigations into the compressive strength of GFRP-RCC columns. Tables 4 and 5 draft the details of some significant literature done in recent years on GFRP-RCC columns. To improve the clarity and readability of the tables, the original layout has been partitioned into two separate tables, referred to as Tables 4 and 5. Table 4 details the rebar type and diameter, cross-sectional characteristics of the column, concrete type and strength, failure modes, and factors that influence the compressive strength of FRP-RCC columns. Tables 5 continues 4, listing the compressive strength (f_{cu}) and ductility values for GFRP-RCC columns compared with conventional steel-reinforced concrete columns under concentric and various eccentric loading conditions.

Table 4 shows that the predominant focus of recent studies has been on GFRP-reinforced concrete columns [37–41, 45–48], with limited investigations conducted on BFRP-reinforced concrete columns [41–44] and CFRP-reinforced concrete columns. This can be attributed to the fact that GFRP is the least expensive composite among FRP materials when compared to BFRP, CFRP, and AFRP rebars, with CFRP being the most expensive, despite only a

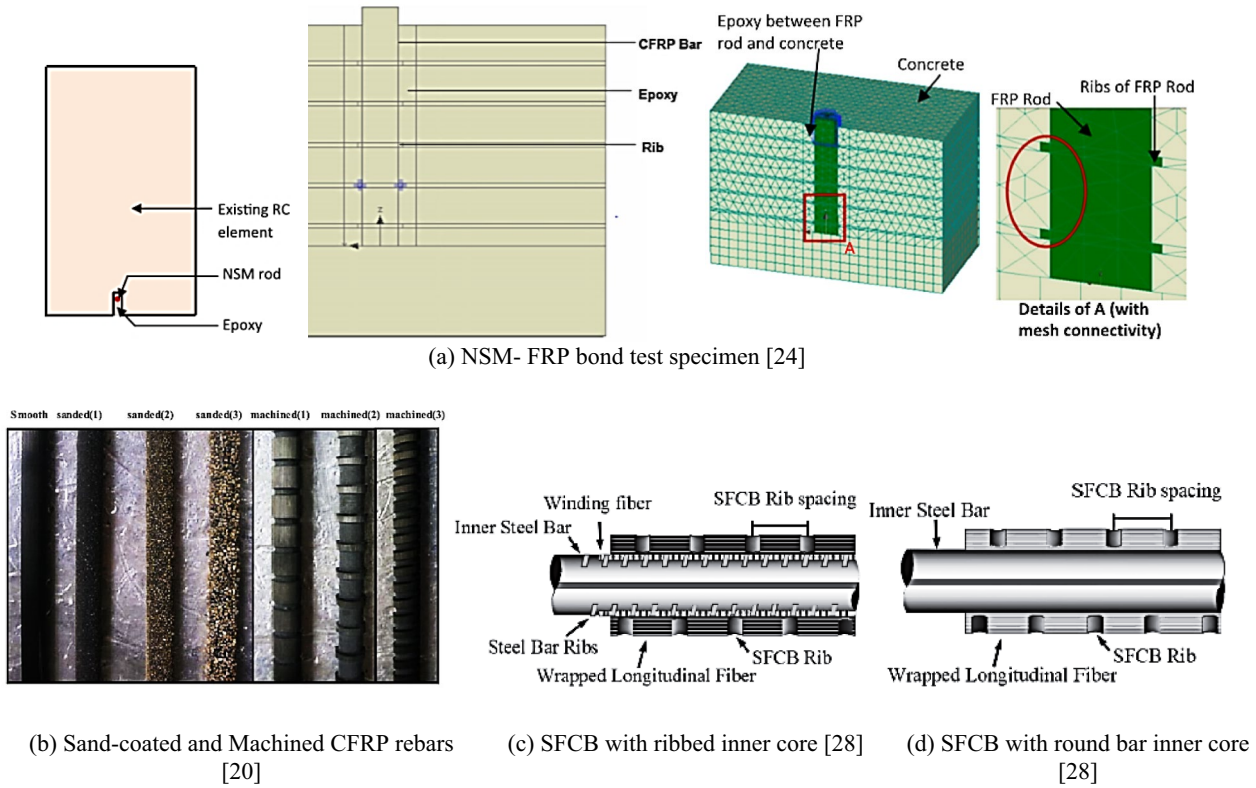


Fig. 2 Various bond mechanisms adopted for bond strength study

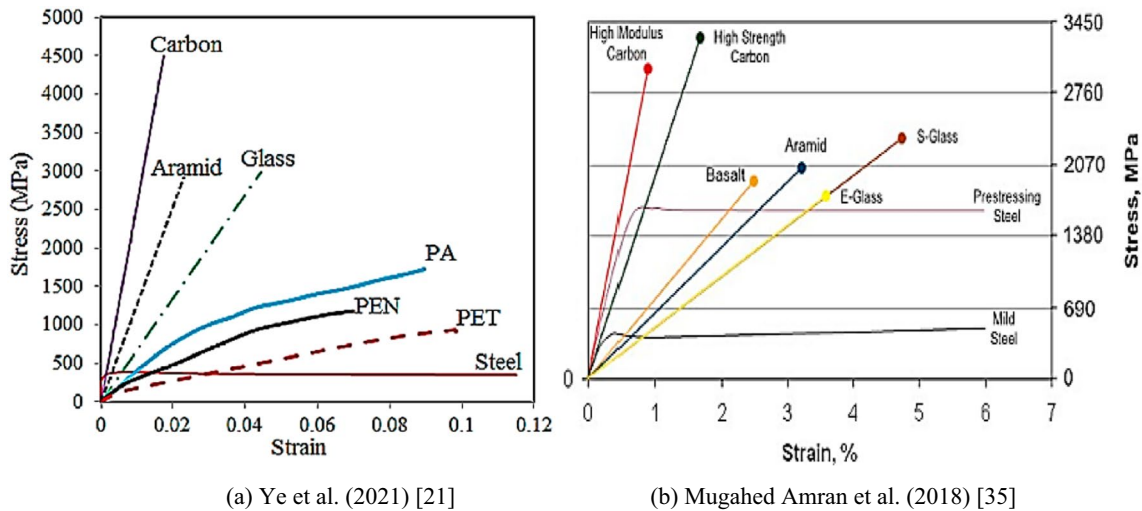


Fig. 3 Typical tensile stress–strain comparison curves of FRP rebars

slight reduction in strength of GFRP rebars relative to BFRP and CFRP rebars [8]. Notably, there is a lack of research on AFRP reinforced concrete columns, as AFRF rebars are not widely used because of their low compressive strength despite their high cost.

The failure modes observed in FRP-RCC columns under concentric loading are similar to those observed in conventional steel-RCC columns. These failure modes include spalling of the concrete cover and crushing of the concrete at the mid-height of the columns [37–43, 47, 48] (refer Fig. 6). Additionally, for Normal Strength Concrete (NSC), there is

Fig. 4 Failure of an FRP rebar under tension, Antino et al. [36]



Table 2 Mechanical properties of rebar material

References	Rebar material	δ (g/cm ³)	E_t (GPa)	f_t (MPa)	E_t (FRP)/ E_t (steel)	f_t (FRP)/ f_t (steel)
Amran et al. [35]	Steel	7.75–8.05	200	500–500	–	–
	GFRP	2.11–2.70	35–51	480–1600	0.2–0.3	1–3.2
	BFRP	2.15–2.70	45–59	1035–1650	0.2–0.3	2.1–3.3
	AFRP	1.28–1.45	41–125	1720–2540	0.2–0.6	3.4–5.08
	CFRP	1.55–1.76	120–580	1720–3690	0.6–2.9	3.4–7.4
Naser et al. [34]	GFRP (13 mm dia)	–	41–42	620–690	–	–
	CFRP (13 mm dia)	–	124	2070	–	–
	AFRP (38 mm dia)	–	70.3	1448	–	–
	BFRP (18 mm dia)	–	35.2	676	–	–
Reichenbach et al. [15]	AR-Glass	2.7	76	2000	0.4	3.6
	Carbon	1.73–1.96	200–500	1750–7000	1–2.4	3.2–12.7
	Basalt	2.75	89	2000–4840	0.4	3.6–8.8
	Steel	7.85	210	550	–	–
Abbood et al. [8]	CFRP	1.50–2.10	37–784	600–3920	0.2–4	1.2–5.7
	GFRP	1.25–2.50	35–86	483–4580	0.2–0.4	1–6.6
	AFRP	1.25–1.45	41–175	1720–3620	0.2–0.9	3.6–5.3
	BFRP	1.90–2.10	50–65	600–1500	0.3–0.3	1.2–2.2
	Steel	7.85	200	483–690	–	–
Ye et al. [21]	CFRP	1.89	398	2600	–	–
	GFRP-Electric-glass	2.6	72	1720	–	–
	GFRP-Strength-glass	2.5	87	2530	–	–
	AFRP	1.43	98	2205	–	–

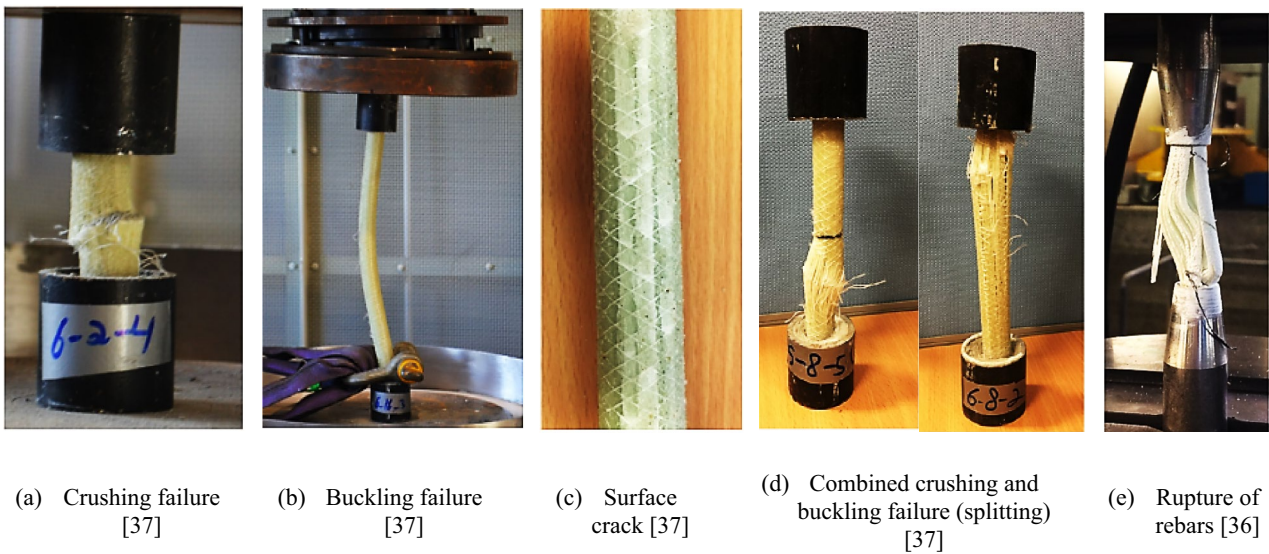
a subsequent occurrence of bar buckling or fracture of the FRP rebar. In contrast, High Strength Concrete (HSC) does not result in any damage to the rebar [37, 41]. In Table 5, the eccentricity of columns is expressed in terms of eccentricity ratio (e/d), which is the ratio of eccentricity (e) to the width or depth (d) of the column's cross-section along the line of application of eccentricity. The failure of FRP-RCC columns under eccentric loading is commonly caused by the formation of vertical cracks and the crushing of the concrete core on the compression face, followed by the yielding of the tensile reinforcement and tension cracking on the tension face [38–42, 44–48] (refer Fig. 7). Furthermore, it has been

noted that GFRP bars and BFRP bars do not buckle even after the concrete core has been crushed [41, 42].

The average compressive strength values for a particular size of reinforcement bars of FRP-RCC columns under different loading conditions are calculated from the compressive load values by dividing the peak compressive load from the cross-sectional area of the columns. This is done to facilitate the comparison of data from different researchers and serve as a concrete grade reference. Table 5 lists the compressive strength separately for experimental and numerical conditions. The table further distinguishes between traditional steel-RCC columns and FRP-RCC columns.

Table 3 Comparison of compressive and tensile strength and elastic modulus of FRP bars

Reference	Rebar (mm)	f_t (MPa)	f_c (MPa)	E_t (GPa)	E_c (GPa)	f_c/f_t	E_c/E_t	
Chaalla et al. [40]	GFRP-12.7	683	492	40	43	0.72	1.08	
	GFRP-15.9	684	525	41	46	0.77	1.12	
	GFRP-19.1	719	577	43	41	0.80	0.95	
Deitz et al. [39]	GFRP-15	–	–	–	–	0.5	1	
Khorramian et al. [38]	GFRP-13	758	559	46	45.78	0.74	1	
	GFRP-16	940	795	42.5	41.16	0.85	0.97	
	GFRP-19	690	684	46	48.89	0.99	1.06	
AlAjarmeh [37]	GFRP-9.5	1315	1319	62.5	70.17	1.00	1.12	
	GFRP-15.9	1237.4	898.6	60	60.24	0.73	1.00	
	GFRP-19.1	1270	890.5	60.5	60.06	0.70	0.99	
D Antino et al. [36]	Thermoset	1091.5	603	48.28	53.92	0.55	1.12	
	GFRP-10	1044	682.33	47.73	47.82	0.65	1.00	
	Thermoset	1206.5	746	48.20	51.55	0.62	1.07	
	GFRP-12	1034	535	53.57	49.41	0.52	0.92	
	Thermoset	1043.5	618	52.81	52.20	0.59	0.99	
	GFRP-16	1031.5	562	52.78	52.13	0.54	0.99	
	Thermoplastic	1034.5	493	52.70	48.36	0.48	0.92	
	GFRP-6	1067	618	52.08	50.44	0.58	0.97	
	Thermoplastic							
	GFRP-8							
	Thermoplastic							
	GFRP-10							
	Thermoplastic							
GFRP-12								
Thermoplastic								
GFRP-16								
Mean						0.69	1.02	
COV						0.23	0.06	

**Fig. 5** Failure modes of FRP rebars under compression

Additionally, Table 5 and Fig. 8 provide information on the strength ratio, denoted as f_{cuFRP}/f_{csteel} , which represents the average compressive strength of FRP-RCC columns (f_{cuFRP}) compared to that of steel-RCC columns (f_{csteel}). This data

aids in comprehending the relative axial strength of both types of columns.

Based on the data presented in Table 5 and Fig. 8, it can be observed that the compressive strength of GFRP-RCC

Table 4 GFRP-RCC column failure modes and compressive strengths based on literature

Ref no	Longitudinal rebars (mm)	Concrete strength (MPa)	Cross-section size × length (mm)	Failure mode	Factors affecting compressive strength
Hasan et al. [43]	GFRP—10	NSC—45.2	Circular 154 Ø × 600	Spalling of concrete cover and buckling of bars in both GFRP and steel-reinforced concrete (refer Fig. 6a)	Rebar and rebar material, compressive strength of concrete
	Steel—10				
	GFRP—13 Steel—10 GFRP—10 Steel—10	HSC—89.5	Similar failures were observed in NSC columns, but the ultimate failure showed no rupture of transverse steel reinforcement and only buckling of GFRP bars (refer to Fig. 7a and 7b)		
Gouda et al. [44]	GFRP—13 Steel—10	NSC—34.7	Circular 305 Ø × 1500	Concrete crushing followed by fracture of GFRP longitudinal bars (refer Fig. 6c) Vertical cracks on the compression side at mid-height and horizontal cracks on the tension side Concrete crushing followed by fracture of GFRP longitudinal bars	Percentage of longitudinal reinforcement, eccentricity ratio
	GFRP—15.9 (Pt-2.5%)				
	GFRP—15.9 (Pt-3.8%)				
Raza et al. [45]	GFRP—12 Steel—12	RAC—38	Circular 300 Ø × 1200	Cracking in the upper portion of columns followed by rupture of main bars Failure of the concrete core on the compression side	Spacing of ties, type of bars, eccentricity ratio
Ali et al. [46]	GFRP—12 Steel—12	RC -PMC—38	Circular 300 Ø × 1200	Buckling of longitudinal rebars, crushing of concrete core and rupture of ties Crushing of concrete core on the shortening side	Use of polypropylene fibres, spacing of ties, eccentricity ratio
Bakouregui et al. [47]	GFRP—15.9 Steel—16	LWSCC—52	Circular 305 Ø × 1500	Concrete cover spalling followed by concrete crushing at mid-column height. BFRP and GFRP reinforcement did not show any damage at peak loads (refer to Fig. 6b)	Level of eccentricity, reinforcement type
ElMessalaj et al. [48]	BFRP—16 Steel—16 BFRP—20	NSC—28.4 (for BFRP ties) and NSC—34.4 (for steel ties)	Square 180 × 180 × 1000	Shearing of the upper and lower segments of the columns after crushing of the core and spalling of concrete cover (refer Fig. 6d)	Spacing of ties, type of ties, eccentricity ratio

Table 4 (continued)

Ref no	Longitudinal rebars (mm)	Concrete strength (MPa)	Cross-section size × length (mm)	Failure mode	Factors affecting compressive strength
Zhang et al. [49]	BFRP—12 Steel—12	NSC—35.2	Square 180 × 180 × 1100	Compression failure and crushing of concrete cover without buckling of longitudinal BFRP bars or rupture of ties	Columns reinforced with hybrid bars have better strength and ductility
Ge et al. [50]	Hybrid (steel and FRP)—12 BFRP—12 Steel—12	NSC—26.86	Rectangular 120 × 180 × 1080	Tensile reinforcement yielded the crushing of concrete on the compression face	Type of rebar material, concrete compressive strength and eccentricity ratio
Hassan et al. [51]	steel-FRP composite—12 Steel—12 GFRP—10 Steel—10	SCC—40	Circular 150 Ø × 600	Vertical cracks appear at the upper and lower regions of the column, and horizontal cracks are observed at mid-height at 0.65Pu. GFRP rebars locally buckle after concrete crushing (refer to Fig. 7c)	Slenderness ratio of the columns, volumetric ratio of the stirrups, and reinforcement material
Salah-Eldin et al. [52]	GFRP—19 Steel—20	HSC—71.2	Circular 150 Ø × 900 Circular 150 Ø × 1200 Square 400 × 400 × 2000	Horizontal tensile cracks, spalling of concrete cover at mid-height, yielding of compression reinforcement (refer Fig. 6e)	Type of rebar material, concrete compressive strength and eccentricity ratio
Elchalakani et al. [53]	GFRP—14	GPC—26	Rectangular 160 × 260 × 1200	Large deformation of the ligatures and longitudinal bar buckling (refer to Fig. 6f)	Rebar arrangement, spacing of stirrups, rebar material and loading conditions
Elchalakani et al. [54]	GFRP—12.7 Steel—12	NSC—32.8		Concrete crushing at compression face, slipping of GFRP bars near the top (refer Fig. 7d)	
				GFRP RCC columns failed due to longitudinal bar buckling and transverse reinforcement rupture, and steel RCC columns failed due to either local buckling or global buckling of rebars	
				Global bending deformation, Tension cracking on tension face (refer Fig. 7e)	

NSC normal strength concrete, HSC high strength concrete, RAC recycled aggregate concrete, RC-PMC polypropylene macro synthetic structural fibre concrete, LWSCC lightweight-aggregate Self-Consolidating Concrete, SCC- Self Compacting Concrete, and GPC- Geopolymer Concrete

columns is within the range of 82% to 100% of the compressive strength exhibited by conventional steel-RCC columns in the case of concentrically loaded columns [43–49, 53, 54]. Similarly, for eccentrically loaded columns, the compressive strength of GFRP-RCC columns ranges from 60 to 103% of conventional steel-RCC columns [44–48, 50–54]. As depicted in Fig. 8, the strength ratio consistently declines as the eccentricity ratio increases from concentrically loaded columns to an eccentricity ratio of 0.2. Furthermore, for eccentricity ratios of 0.3 or higher, the compressive strength of GFRP-RCC columns slightly surpasses that of steel-RCC columns. This may be attributed to the condition that the columns fail under combined bending and compression when the eccentricity ratio exceeds 0.3. In this case, the steel bars yield, preventing flexural strength development, whereas the FRP bars gain strength till their maximum load. Thus, GFRP bars with a higher tensile strength than steel bars, especially on the tension face of columns under eccentric pressure, can resist load more than their steel counterparts [52, 54]. El Messalami et al. [48] added that ignoring the contribution of increased strength due to increased ductility could underestimate the ultimate capacities of BFRP-RCC columns by an average of 33%. Xiong et al. [41] investigated the compressive strength of BFRP-reinforced seawater sea-sand concrete square column. The findings suggest that reducing tie spacing can enhance the compressive strength of concrete and offer strong resistance to corrosion caused by seawater, thereby improving the durability of the columns. The post-peak compressive strength of the square GFRP-RCC columns was increased by using spiral stirrups to confine the longitudinal GFRP rebars further, and this type of GFRP-RCC can be used in marine engineering, according to Fang et al. [42].

Ductility

The primary purpose of considering the ductility of building structures is to ensure that they possess a specific capacity for energy dissipation and deformation. This characteristic is crucial in mitigating the risk of sudden brittle damage caused by earthquakes and strong winds. Ductility refers to the capacity of a column to undergo plastic deformation when subjected to compressive stress until it reaches the point of failure [44, 55]. An alternative interpretation of ductility pertains to the amount of energy absorbed by column specimens after reaching their maximum load [54]. The measurement of column ductility is typically quantified using a ductility index, which can be expressed concerning different variables, including energy absorption or dissipation, compressive deformation or shortening, and curvature or rotation of the structures [45, 51, 54]. The ductility index

of GFRP or steel-reinforced concrete columns has been determined using the following approaches as stated below:

- DI_1 -Ratio of the area under the load–displacement curve up to 3 times yield deformation point by yield deformation point [43, 56, 57].
- DI_2 -Area under the load–displacement curves corresponding to ultimate displacement at reinforcement rupture by area corresponding to yield displacement [44, 58, 59].
- DI_3 -Ultimate displacement (corresponding to $0.85P_u$) by Yield displacement, P_u is peak load [45, 46, 48, 60–62].
- DI_4 -Area under the load–deflection curve up to $0.85P_u$ on the post-peak collapse curve by Area under the load–deflection curve up to $0.75 P_u$ [47, 62].
- DI_5 -Area under the load–deflection curve up to peak load by Area under the load–deflection curve before load decreases to $0.25P_u$ [51, 54, 63].

Based on loading conditions and rebars of a particular size, the ductility indexes are averaged and specified separately for traditional steel-RCC columns and FRP-RCC columns in Table 5. The ductility index ratios of GFRP-RCC columns to that of steel-RCC columns are listed in Table 5 and Fig. 9.

It is observed that for most of the cases, the ductility index of FRP-RCC columns under any loading condition or concrete type is higher than steel-RCC columns. From the data available in Table 5 and Fig. 9, the average percentage increase in ductility of FRP-RCC columns is calculated to be 13.6%, and that of GFRP-RCC columns is 17.4% with a maximum increase of 44.2% for BFRP-RCC columns [48] and 35.5% for GFRP-RCC columns [43]. Numerous authors have provided plausible rationales for the observed increase in the ductility index. Hasan et al. [43] hypothesised that after yielding in the first peak, the contribution for steel rebars remains nearly the same. In contrast, GFRP's higher tensile strength and the possibility of axial load transformation into eccentric axial load due to lateral deformation experienced by these specimens during testing leads to more excellent energy absorption of the GFRP-RCC column specimens. Gouda et al. [44] have suggested a similar rationale, stating that an increase in the longitudinal reinforcement ratio and eccentricity significantly improves energy absorption ability, resulting in a higher ductility factor. Furthermore, an alternative explanation proposed by Raza et al. [45] is that the variability in the ductility capacity of GFRP-RCC columns can be attributed to the complex performance of GFRP bars under compression. Similarly, ElMessalami et al. [60] recommended the use of GFRP-RCC columns in seismically active zones due to their higher ductility than steel-RCC columns, claiming that GFRP-RCC columns

Table 5 Compressive strength and ductility of RCC columns reinforced with FRP and steel rebars

Ref no	Longitudinal rebars (mm)	Type of loading		f_{cu} (MPa)		Ductility index		f_{cuFRP}/f_{csteel}	Ductility ratio		
		Experimental	FEA	Experimental		FRP				Steel	
				FRP	Steel	FRP	Steel			FRP	Steel
Hasan et. al. [43]	GFRP—10	Concentric	42.57, 71.59*	47.46		DI ₁ —5.81, 14*	DI ₁ —5.07, 10.7*	0.89, 1.51 ^a	1.15, 1.31 ^a		
	Steel—10										
	GFRP—13		46, 74.95*			DI ₁ —5.94, 14.5*		0.96, 1.57 ^a	1.17, 1.36 ^a		
	Steel—10			97.22				0.92			
	GFRP—10		89.68								
Gouda et al. [44]	GFRP—13		98.14					1			
	Steel—10										
	GFRP—15.9 (Pt-2.5%)	Concentric	37.76			DI ₂ —2.3					
		Eccentric (e/d-0.08, 0.16, 0.33, and 0.66)	30.94, 24.59, 12.22, and 5.23			DI ₂ —1.8, 3.4, 4.7, and 4.8					
	GFRP—15.9 (Pt-3.8%)	Concentric	39.66			DI ₂ —3.4					
Raza et al. [45]	GFRP—12	Eccentric (e/d-0.08, 0.16, 0.33, and 0.66)	31.73, 24.59, 14.75, and 6.66			DI ₂ —2.3, 3.5, 6.9 and 6.8					
	Steel—12										
	GFRP—12	Concentric	34.28	41.97	33.84	DI ₃ —2.83	DI ₃ —2.52	0.82	1.12		
		Eccentric (e/D* -0.1, and 0.2)	24.62, and 15.18	29.98, and 19.19	23.76, and 15.1	DI ₃ —2.79, and 2.82	DI ₃ —2.19 and 2.55	0.82, and 0.79	1.27, and 1.11		
	Steel—12										
Ali et al. [46]	GFRP—12	Concentric	35.84	43.57		DI ₃ —2.69	DI ₃ —2.36	0.82	1.14		
	Steel—12					DI ₃ —2.89, and 2.82	DI ₃ —2.19 and 2.55	0.83, and 0.79	1.32, and 1.11		
	GFRP—15.9	Concentric	48.31	53.38		DI ₄ —2.93	DI ₄ —3.1	0.91	0.95		
Bakouregui et al. [47]	Steel—16	Eccentric (e/D-0.33)	6.02	7.73		DI ₄ —1.91	DI ₄ —1.98	0.78	0.97		
	BFRP—16	Concentric	48.31	53.38		DI ₄ —2.29	DI ₄ —3.1	0.91	0.74		
ElMessalai et al. [48]	Steel—16	Eccentric (e/h-0.22, and 0.66)	13.89, and 6.23	17.66, and 7.73		DI ₄ —1.96, and 1.89	DI ₄ —1.95, and 1.98	0.79, and 0.78	1, and 0.96		
	BFRP—20	Concentric	26.19	33.33 (steel ties)		DI ₃ —3	DI ₃ —2.08	0.79	1.44		
	Steel—16	Eccentric (e/h-0.22, and 0.44)	16.52, and 10.01	22.22, and 12.71 (steel ties)		DI ₃ —2.96, and 1.37	DI ₃ —2.3, and 1.81	0.74, and 0.79	1.29, and 0.76		

Table 5 (continued)

Ref no	Longitudinal rebars (mm)	Type of loading	f_{cu} (MPa)		Ductility index		f_{cuFRP}/f_{csteel}	Ductility ratio
			Experimental		FEA			
			FRP	Steel	FRP	Steel		
Zhang et al. [49]	BFRP—12 Steel—12	Concentric	26	31.4			0.83	
	Hybrid (steel and FRP)—12		30.1				0.96	
Ge et al. [50]	BFRP—12 Steel—12	Eccentric (e/d-0.5, e/d-0.83)	10.88, and 5.19	16.44, and 8.56			0.67, and 0.60	
	steel-FRP composite—12	Eccentric (e/d-0.5, e/d-0.83)	11.11 and 6.02				0.68, and 0.70	
Hassan et al. [51]	GFRP—10 Steel—10	Eccentric (e/d-0.2)	27.05 25.53	34.68 33.29			0.78 0.77	1.07 1.21
			24	31.49			0.76	1.11
Salah-Eldin et al. [52]	GFRP—19 Steel—20	Eccentric (e/h ^{***} -0.2, 0.3, 0.4, and 0.6)	31.88, 22.63, 15.36 and 8.54	32.11, 26.33, 18.87 and 8.36			0.99, 0.86, 0.81 and 1.02	
Elchalakani et al. [53]	GFRP—14	Concentric	28.78		29.67			
		Eccentric (e/d-0.16, 0.22, and 0.3)	17.56, 9.7, and 5.75		16.7, 8.40, and 4.24			
Elchalakani et al. [54]	GFRP—12.7 Steel—12	Concentric	33.8	37.92	36.12		0.89	1.30
		Eccentric (e/d-0.16, 0.22, and 0.3)	21.60, 18.94, and 14.04	22.44, 19.59, and 13.62	23.5, 21.20 and 13.67		0.96, 0.97, and 1.03	1.30

*Second peak load

**D is the diameter of a column having a circular cross-section

***h is column width



(a) Spalling of concrete cover [43]

(b) Concrete crushing at mid-height [47]

(c) Fracture of bars [44]



(d) Shearing of the upper and lower sections of columns [48]

(e) Horizontal tensile cracks [52]

(f) Deformation of ligatures and longitudinal bar buckling [53]

Fig. 6 Failure of GFRP-RCC columns under concentric loading

absorb more energy through their flexibility and capability of deforming well in the post-peak collapse region.

In summary of the observations from the literature review on the ductility of GFRP-RCC columns and compressive strength of FRP rebars, the enhancement in ductility exhibited by FRP-RCC columns compared to

conventional steel-RCC can be attributed to distinct failure mechanisms of the steel and FRP rebars. In the case of steel rebars subjected to compressive failure, buckling of the steel bar occurs. Conversely, in the case of FRP rebars subjected to compressive failure, the initial loss of bond between the fibres and matrix is followed by subsequent



(g) Crack distribution at mid-height of column [49]

Fig. 6 (continued)

buckling of individual strands or select groups of fibres. Ultimately, this sequential buckling process culminates in the bars' rupture, failing all fibres or groups of fibre strands. Hence, after experiencing yielding or buckling during the initial peak, the steel rebars exhibit a relatively consistent contribution. In contrast, the GFRP rebars require a longer duration due to their complex failure mechanism when subjected to compression. Furthermore, the higher tensile strength of GFRP bars and the possibility of axial load transformation into eccentric axial load due to lateral deformation experienced by RCC column specimens during testing results in more excellent energy absorption by GFRP-RCC column specimens. However, to confirm this justification, additional research is necessary to validate this finding.

Effect of key parameters on compressive strength and ductility of GFRP-RCC columns

The concrete strength, rebar type, percentage of longitudinal reinforcement, spacing of ties, eccentricity ratio, and slenderness ratio of columns are crucial parameters that affect the compressive strength of FRP-RCC columns [43–54]. These parameters can be considered in future research experiments and analysis of FRP-RCC columns. The subsequent section examines the impact of these factors on the strength and ductility of GFRP-RCC columns compared to conventional steel-RCC columns based on a comprehensive study of existing literature.

Shape of column

The strength and ductility of a column can be influenced by the shape of its cross-section [64]. Figures 10 and 11 depict a comparison of the strength and ductility of GFRP-RCC columns to steel-RCC columns. Figure 10 displays the percentage strength ratio ((f_{FRP}/f_{steel}) (%)) of GFRP-RCC columns compared to steel-RCC columns for circular, square, and rectangular cross-sectional shapes. The specimen IDs are assigned such that the first letter 'C', 'S' and 'R' represent Circular, Square and rectangular cross-sections. This is followed by a hyphen and a number showing the value of the eccentricity ratio, which, if denoted as '0', is considered a concentrically loaded column. Lastly, square brackets indicate the literature reference number. For example, C-0 [43] represents circular cross-section reinforced concrete columns loaded concentrically and data is taken from Hasan et al. [43].

Figure 10 demonstrates that both circular and square GFRP-RCC columns exhibit a decrease in strength ratio (%) as the loading eccentricity increases. However, square columns with an eccentricity ratio of 0.6 maintain the same strength as their steel counterparts. Contrarily, the strength ratio of a rectangular cross-section concrete column increases as the loading eccentricity increases. At an eccentricity ratio of 0.3, it reaches almost 103% of the strength of its steel-reinforced column counterpart [54]. In the case of concentric loading, the shape of columns has minimal impact on the strength ratio (%), and GFRP-RCC columns give an average compressive strength of 89% compared to steel-RCC columns. Figure 11 shows that regardless of the column shape, the ductility index of GFRP-RCC columns is on par with its steel-RCC counterpart.

Type of concrete

The type and grade of concrete are other factors that can affect the compressive strength and ductility of FRP-RCC columns. Figures 12 and 13 depict a comparison of the strength and ductility of GFRP-RCC columns to steel-RCC columns based on the type and grade of concrete. Figure 12 displays percentage strength ratio ((f_{FRP}/f_{steel}) (%)) of GFRP-RCC columns compared to steel-RCC columns for Ordinary Portland cement concrete (OPC), Recycled Aggregate Concrete (RAC), Polypropylene macro synthetic structural fiber concrete (PMC), Self Compacting Concrete (SCC), Lightweight-aggregate self-consolidating concrete (LWSCC), Normal Strength Concrete (NSC) and High Strength Concrete (HSC) columns. The specimen IDs are structured such that the initial letter denotes the concrete type, followed by a hyphen, and then the compressive strength or grade of concrete in MPa is indicated. After the hyphen, there is a number that represents the eccentricity ratio. If this value



(a) Vertical crack on the compression side [44]



(b) Horizontal cracks on the tension side [44]



(c) Vertical cracks in upper and lower regions and horizontal cracks at mid-height [51]



(d) Slipping of GFRP rebars near the top [53]



(e) Global bending [54]

Fig. 7 Failure of GFRP-RCC columns under eccentric loading

is '0', it suggests that the column is loaded concentrically. Lastly, the reference number of literature from which the data is taken is given in square brackets. For instance, SCC-40-0.2 [51] represents self-compacting reinforced concrete columns with a concrete grade 40 MPa, loaded eccentrically

with an eccentricity ratio of 0.2, and data is taken from Hassan et al. [51].

For columns subjected to axial compression, HSC columns exhibit strength comparable to steel-RCC columns. On the other hand, NSC columns demonstrate approximately 93% of the strength of steel-RCC columns [43]. The average

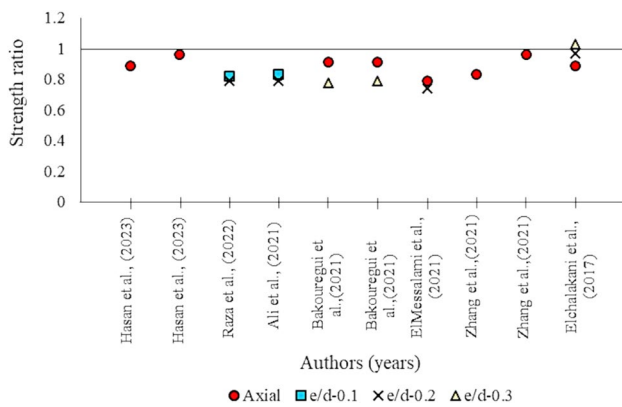


Fig. 8 Strength ratios of GFRP versus steel-reinforced columns

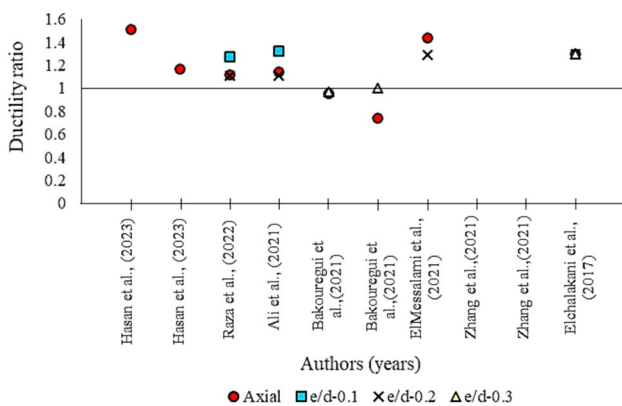
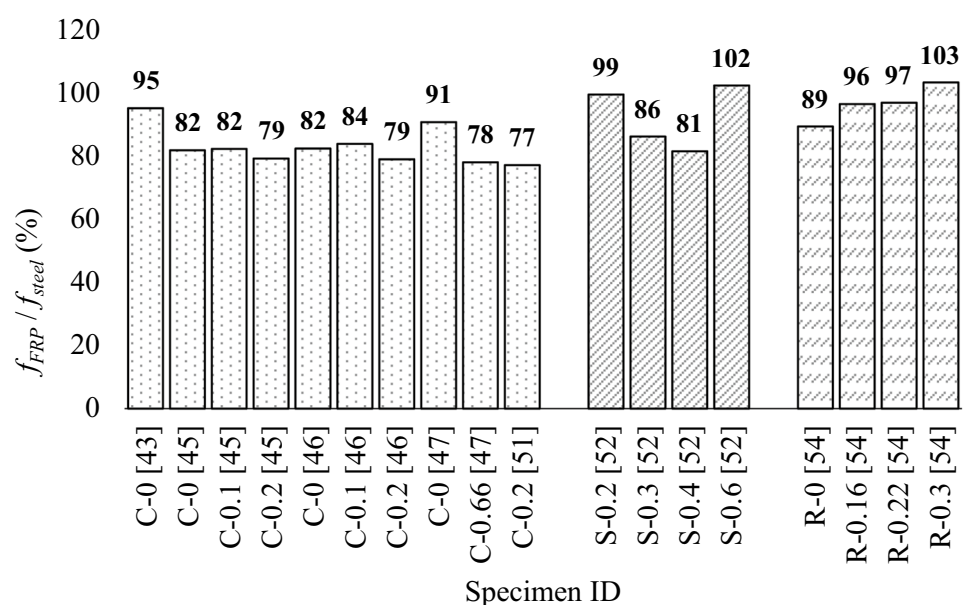


Fig. 9 Ductility ratios of GFRP versus steel-reinforced columns

Fig. 10 Percentage strength comparison of GFRP-RCC columns based on cross-section shape

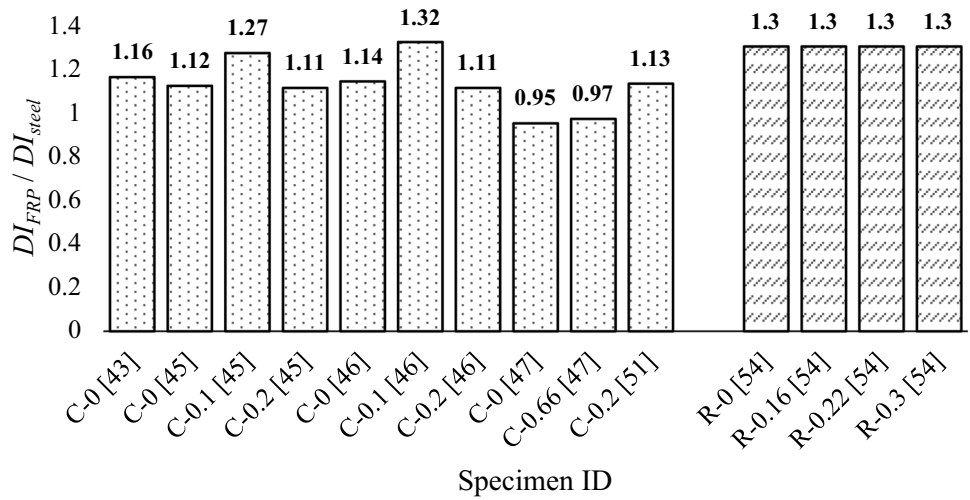


percentage strength ratio of GFRP-RCC columns is ranked in the following order: 97% for HSC, 93% for NSC, 91% for LWSCC, 89% for OPC, and 82% for both RAC and PMC columns, as seen in Fig. 12. The percentage strength ratio of HSC, NSC, LWSCC, OPC, RAC, and PMC columns reinforced with GFRP longitudinal bars decreases as the eccentricity increases. HSC columns (having an eccentricity ratio of 0.6) and OPC concrete columns show an increase in percentage strength ratio with increasing eccentricity ratio. Irrespective of the type and grade of concrete, the ductility of GFRP-RCC columns is higher than steel reinforced concrete columns except for the LWSCC type of concrete, where the strength and ductility are almost the same as its steel counterpart. The ductility index of GFRP-RCC columns with OPC concrete remains constant regardless of the eccentricity ratio [54]. Compared to their steel bar-reinforced NSC counterparts, GFRP bar-reinforced NSC column specimens have better ductility; however, the opposite was observed for column specimens cast with HSC [43].

Slenderness ratio of columns

As per ACI318-19 [65] and IS456-2000 [66], if the ratio of the length of the column to its least lateral dimension (L/D) is less than 12, then the column is classified as short or stub column; otherwise, it is classified as long or slender columns. The L/D ratio (slenderness ratio) can be considered as one of the factors that might influence the compressive strength and ductility of GFRP-RCC columns. Figures 14 and 15 display a comparison of the strength and ductility of GFRP-RCC columns to steel-RCC columns based on the different L/D ratios. The specimen IDs are named such

Fig. 11 Ductility index comparison of GFRP-RCC columns based on cross-section shape



that the first part shows the *L/D* ratio followed by a hyphen and a number that indicates the eccentricity ratio, which, if denoted as '0', is considered a concentrically loaded column. Lastly, the data's source literature reference number is provided in square brackets. For example, L/D-4-0 [43] represents a column with an *L/D* ratio of 4, which is loaded concentrically, and data is taken from Hasan et al. [43].

For the case of columns subjected to axial compression, with the increase in *L/D* ratio, the percentage strength ratio of GFRP-RCC columns decreases. GFRP-RCC columns have varying strengths for distinct eccentricity ratios; nonetheless, their relative strength tends to rise as the eccentricity ratio increases, with the exception of cases where the *L/D* ratio is greater than 8 [54]. Hassan et al. [51] examined the compressive strength and ductility of RCC columns that

were reinforced longitudinally with GFRP and steel bars and transversely with steel spiral hoops. Additionally, certain specimens were externally constrained using FRP tubes. It was discovered that as the slenderness ratio increases, the ductility and compressive strength of the steel hoops reinforced concrete columns and the GFRP tubes constrained concrete column specimens decrease. Also, it can be seen from the data provided by the author that for specimens having GFRP longitudinal bars and transverse steel ties (G2), there is an increase in the ductility index of GFRP rebar-reinforced specimens with the rise in the slenderness ratio from 4 to 8. In comparison, a decrease in the value of the ductility index is observed for steel-reinforced column specimens with an increase in the slenderness ratio from 4 to 6. Hence, as seen in Fig. 15, the comparative ductility ratio

Fig. 12 Percentage strength comparison of GFRP-RCC columns based on concrete grade and type

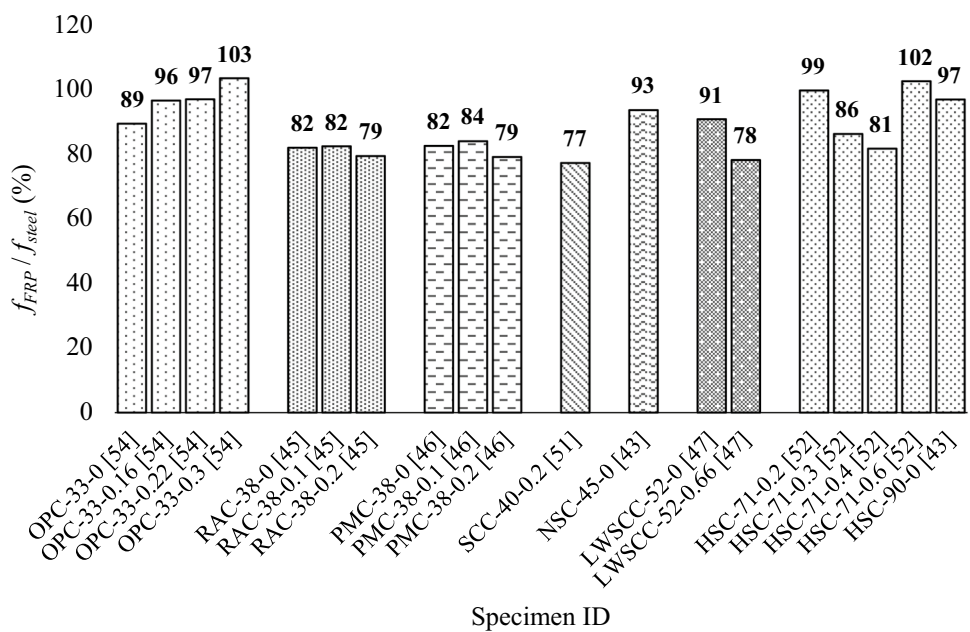
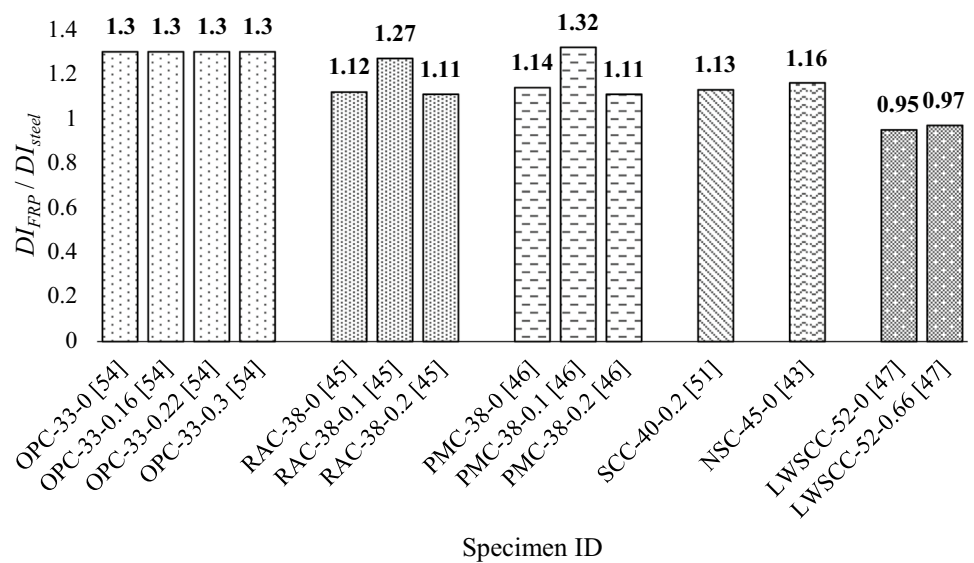


Fig. 13 Ductility index comparison of GFRP-RCC columns based on concrete grade and type



(DI_{FRP}/DI_{steel}) increases, having values of 1.07, 1.21, and 1.11 for slenderness ratios 4, 6 and 8, respectively.

From the given literature, the average value of ductility ratio (DI_{FRP}/DI_{steel}) is 1.2, 1, 1.2, and 1.3 for columns having L/D ratios of 4, 5, 6 and 8, respectively. This demonstrates that for L/D ratios ranging from 4 to 8, GFRP-RCC columns have superior ductility than steel RCC columns. This rise in ductility index is only observed when the replacement of steel longitudinal bars with GFRP as longitudinal bars is done while keeping other parameters the same. Based on this, the authors propose doing additional sets of tests on columns with varying slenderness ratios in order to arrive at a definitive conclusion.

Longitudinal reinforcement ratio

The ratio of Longitudinal reinforcement ($p_l\%$) is considered one of the most crucial parameters that affect the compressive strength and ductility of RCC columns. Figures 16 and 17 below compare the strength and ductility of GFRP-RCC columns relative to steel-RCC columns based on the diameter of the longitudinal bar and the percentage of longitudinal reinforcement ($p_l\%$). The specimen IDs are kept such that the first part shows the bar diameter and $p_l\%$ value followed by a hyphen and a number showing the eccentricity ratio, which, if denoted as '0', is considered a concentrically loaded column. Lastly, the reference number of literature from which the data is taken is given in square brackets. For example, $\varnothing 10$ -Pt-2.4%-0 [43] represents a column having a 10 mm diameter of the longitudinal bar and 2.4% longitudinal reinforcement ratio, which is loaded concentrically during testing and data is taken from Hasan et al. [43].

Figure 16 shows that for concentric loading, the strength of GFRP-RCC columns compared to steel-RCC

columns increases with a higher percentage of longitudinal reinforcement. As the reinforcement percentage (P_l) increases from 0.96 to 2.4%, the strength ratio rises from 82 to 95%. Therefore, along with an increase in strength capacity, as the P_l increases, the comparative strength ratio of GFRP-RCC columns to steel-RCC columns also rises, making the strength of GFRP-RCC columns almost equal to that of steel-RCC columns. The same cannot be said for eccentrically loaded concrete columns, as their relative percentage strength capacity varies, and further research may be required in this area.

Gouda et al. [44] examined the ductility and strength capacity of GFRP-RCC columns with varying longitudinal reinforcement diameters and ratios (Pt). It was observed that increasing bars for the test specimens from 8 to 12 reduced strength deterioration beyond the peak load, which can be explained by the GFRP bars' contributions to confinement. As the longitudinal reinforcement ratio and eccentricity increased, the energy absorption capacity improved significantly, resulting in a higher ductility index. Furthermore, since crack width is inversely related to the maximum spacing between bars, raising the longitudinal reinforcement ratio from 2.5 to 3.8% as a function of number of bars decreased both the average crack spacing and crack width. Hasan et al. (2023) [43] tested NSC and HSC columns reinforced longitudinally with steel bars ($P_t = 2.4\%$) and GFRP bars ($P_t = 0, 2.7, 3.2,$ and 4.3%). Test results show that the axial load supported by the GFRP bar-reinforced NSC column specimens rose as the GFRP longitudinal reinforcement ratio increased. The contribution of GFRP bars accounted for about 50% of the contribution of steel bars in the axial load-carrying capacity of both NSC and HSC specimens.

Fig. 14 Percentage strength comparison of GFRP-RCC columns based on *L/D* ratio

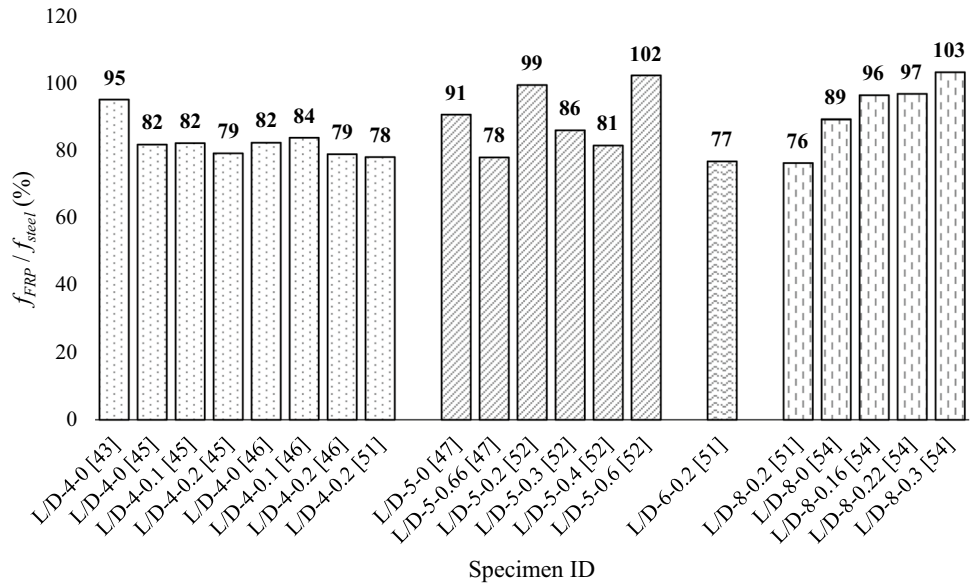
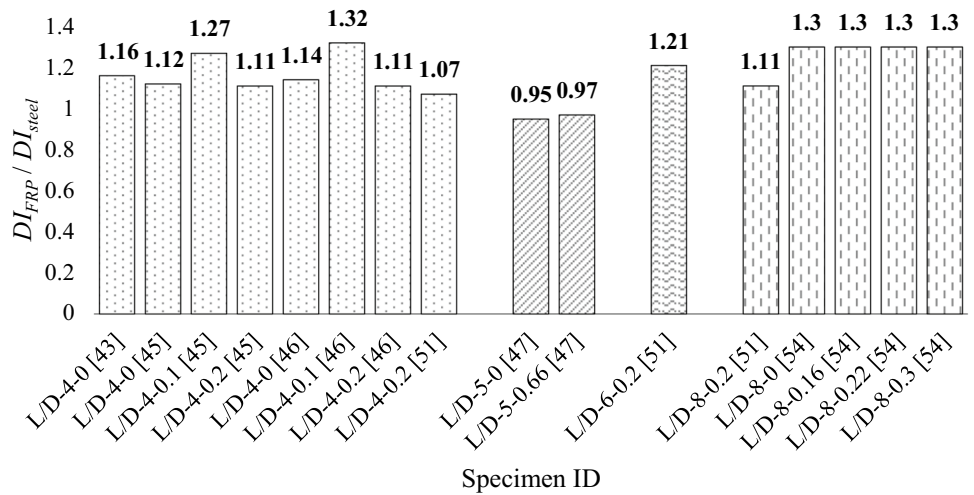


Fig. 15 Ductility index comparison of GFRP-RCC columns based on *L/D* ratio



Transverse reinforcement

The spacing or volume of transverse reinforcement is considered another crucial parameter that affects the compressive strength, ductility and confinement efficiency of RCC columns. Elchalakani et al. [54] tested 17 rectangular GFRP RCC and steel RCC column specimens having different ligature spacing (from 150 to 75 mm) and concrete cover (20 mm and 40 mm) and reported essential results. Reducing the spacing of ties from 150 to 75 mm improves the load-carrying capacity and ductility of GFRP RCC columns. It is recommended not to use larger tie spacing in GFRP-RCC columns, as it can lead to local buckling of the GFRP longitudinal bars, making their contribution to the ultimate load capacity almost negligible. Elchalakani et al. [53] tested GFRP GPC and OPC concrete columns under concentric

and eccentric axial loading having different ligature spacing from 75 to 250 mm. It was observed that as the stirrup spacing was increased, the GFRP bars in GFRP-RCC columns experienced local buckling failure under concentric loading, while slip failure occurred at the plastic hinge in GPC columns loaded with high eccentricity. In contrast, a decrease in the spacing of stirrups in GFRP RCC columns leads to the occurrence of longitudinal bar rupture.

In their study, Hassan et al. (2019) [51] found that increasing the volumetric ratio of the stirrups from 1.7 to 3.4% leads to a 20% increase in the column capacity, irrespective of the type of longitudinal reinforcement. Ali et al. [46] and Raza et al. [45] reported that GFRP-RCC and steel-RCC specimens showed enhanced strength as a result of reducing the spacing between transverse reinforcement. The reduction in pitch from 250 to 150 mm and 150 mm to 75 mm resulted

in strength improvements of 4.7% and 5.8%, respectively, for concentrically loaded GFRP-RCC columns. In contrast, for concentrically loaded steel-RCC columns, the reduction in pitch from 250 to 150 mm and 150 mm to 75 mm led to strength improvements of 2.84% and 13.44%, respectively.

Figures 18 and 19 below compare the strength and ductility of GFRP-RCC columns relative to steel-RCC columns, respectively, based on the diameter of the transverse bar used and the percentage volume of transverse reinforcement. The specimen IDs are kept such that the first part shows the bar diameter and percentage volume of ties followed by a hyphen and a number showing the eccentricity ratio, which, if denoted as '0', is considered a concentrically loaded column. Lastly, the reference number of literature from which

the data is taken is given in square brackets. For example, $\varnothing 10-0.38\%-0.1$ [45] represents a column having a 10 mm diameter of transverse bar, and 0.38% percentage volume of transverse reinforcement, which is loaded eccentrically during testing and data is taken from Raza et al. [45].

In the case of concentric loading, as depicted in Fig. 18, GFRP-RCC columns exhibit a consistent percentage strength ratio. Specifically, for any given percentage volume of ties, GFRP-RCC columns demonstrate about 81% of the strength of steel-RCC columns when using 10 mm diameter ties and 94% of the strength when using 6 mm diameter ties. This shows that although increasing the confinement volume of ties increases the strength capacity of columns, it doesn't have much of an impact on the increase in the relative

Fig. 16 Percentage strength comparison of GFRP-RCC columns based on longitudinal reinforcement ratio

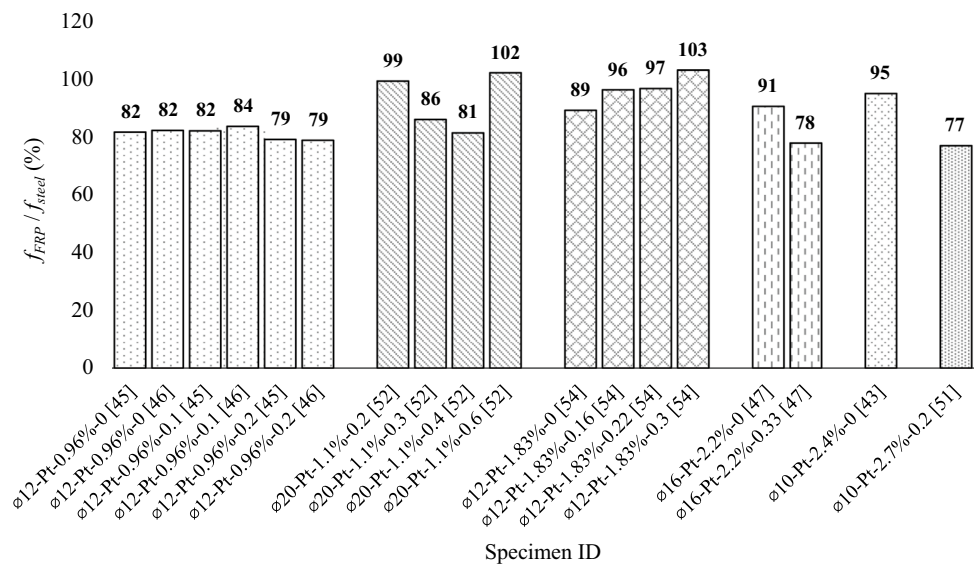
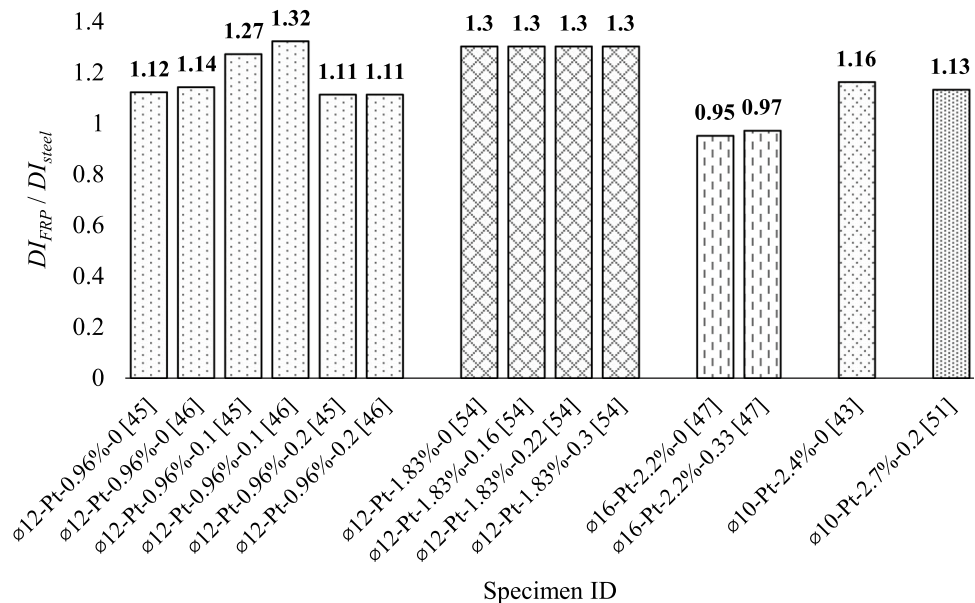


Fig. 17 Ductility index comparison of GFRP-RCC columns based on longitudinal reinforcement ratio



strength of GFRP-RCC columns compared to steel-RCC columns. Additionally, a smaller diameter of ties (6 mm) results in a higher relative strength value for GFRP-RCC columns, nearly equivalent to that of steel-RCC columns. As seen in Fig. 19, the relative ductility index of FRP-RCC columns compared to steel-RCC columns reduces from 1.5 to 1 as the percentage volume of stirrups increases from 0.38 to 1.22%. This is because reducing the spacing of stirrups makes the steel-RCC columns more ductile.

When subjected to eccentric loading with eccentricities ranging from 0.1 to 0.3, GFRP-RCC columns with smaller diameter ties (6 mm) exhibit a higher relative strength compared to concentrically loaded columns. Furthermore, in most instances, the strength of GFRP-RCC columns with 6 mm ties matches that of steel-RCC columns. Eccentric loading does not have a significant impact on the relative strength of GFRP-RCC columns. The comparison of the ductility index between GFRP-RCC columns and steel-RCC columns under eccentric loading does not reveal a substantial change with an increase in the volume of ties. However, it is observed that the ductility index of GFRP-RCC columns is either equal to or greater than that of steel-RCC columns in all cases.

Design equations and numerical methods for predicting the compressive strength of GFRP-RCC columns

The maximum axial load-carrying capacity, P_d of conventional steel bar reinforced concrete columns under concentric axial load can be predicted using Eq. (1) [67], where the contribution of concrete (P_c) and longitudinal bars (P_{bar}) is considered and added together to get the axial load-carrying capacity of columns. Over the years,

researchers have proposed various equations to predict the maximum axial load-carrying capacity of columns made of concrete reinforced with FRP bars [68–78]. The contribution of the concrete to the analytically determined axial load-carrying capacity of FRP bar-reinforced concrete columns is consistent across all the proposed equations. In other words, the variations in the analytically calculated values of P_d for FRP bar reinforced concrete columns can be mainly attributed to the diverse approaches employed in determining the contribution of the FRP longitudinal bars.

Although several researchers have proposed different values for the contribution of GFRP bars in compression, design codes have not offered any pertinent recommendations. The CAN/CSA S806-12 [69] standard does not take into account the contribution of the compressive bars in both flexural and compression members. The reason for this is that the FRP bar's ultimate compressive strength is significantly lower than its ultimate tensile strength. Notably, the average compressive strength of the GFRP bars was 70% of their tensile strength. Zadeh et al. [70] suggested that GFRP may be substituted with a concrete area of the same size during analysis in order to simplify the process. Hence, the existing design standards limit the utilisation of FRP bars in structural elements subjected to compression or in the compression region of elements subjected to bending. However, some research has indicated that GFRP bars, when used as longitudinal reinforcement, accounted for around 3% to 14% of the overall axial load supported by the GFRP-RCC columns [43].

Due to the variations in the reported ultimate compressive strength of the FRP bars and their influence on RCC columns, it was necessary to establish design guidelines to incorporate FRP bars as longitudinal reinforcement in concrete compression members like concrete columns. The ACI 440.1R-15 [71] report emphasises the necessity for

Fig. 18 Percentage strength comparison of GFRP-RCC columns based on the volume of transverse reinforcement (%)

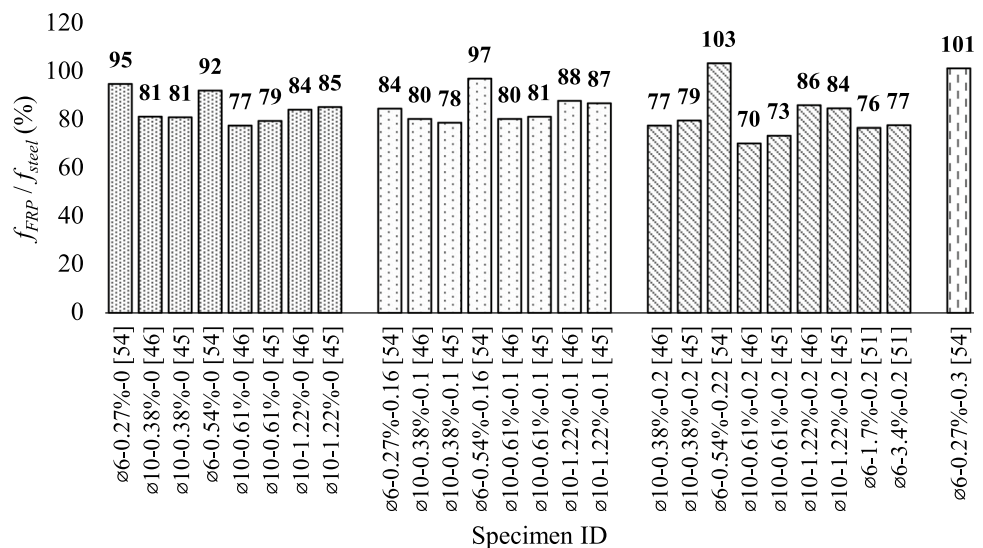
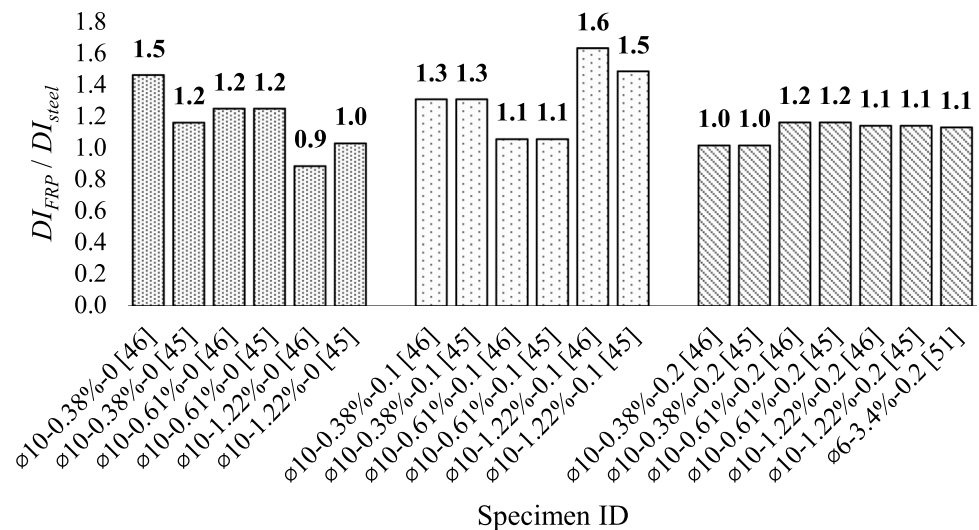


Fig. 19 Ductility index comparison of GFRP-RCC columns based on the volume of transverse reinforcement (%)



further comprehensive investigation of concrete columns. In this regard, experimental and analytical research studies were undertaken to explore and comprehend the behaviour of concrete columns reinforced longitudinally with GFRP bars. Table 6 represents the design equations (Eqs. 1–10) predicted for computing the axial load-carrying capacity of steel-RCC columns and FRP-RCC columns proposed by various researchers over the years. According to Hasan et al. [43], the axial load-carrying capacity of FRP-RCC columns (Eq. 2) is underestimated when the contribution of FRP bars is neglected. This phenomenon is more pronounced in normal-strength concrete columns because FRP bars contribute more significantly to their axial load capacity compared to high-strength concrete columns.

Tobbi et al. [73] mentioned that unlike concrete, which can reach its crushing strain, GFRP bars could not achieve their ultimate strength and recommended a reduction factor for the tensile strength of GFRP bars in relation to the contribution of GFRP bars to the axial load-carrying capacity of GFRP-RCC columns. Hales et al. [75], Hadi et al. [62] and Hadhood et al. [78] (Eqs. 6–7 and 9) used the product of concrete crushing strain and modulus of elasticity of GFRP bars in the design equation of load carrying capacity of FRP-RCC columns. Hasan et al. [72] introduced a new design equation (Eq. 10) for determining the maximum axial load-carrying capacity of GFRP-RCC columns under axial compression, comparing it with equations from previous studies [62, 73–76, 78]. It has been observed that computing the contribution of FRP longitudinal bars using the modulus of elasticity provides better logical predictions compared to calculating the contribution based on the ultimate strength of FRP bars. The reason behind this is that the elastic modulus of FRP bars is nearly identical in both tension and compression. Additionally, it was discovered that employing

a concrete compressive strain-based empirical equation to estimate the axial strain in the FRP longitudinal bars in concrete columns yields better predictions of the role played by the longitudinal FRP bars in the axial load supported by the FRP-RCC columns. The design based on eccentric compression behaviour, which involves complex moment and shear interactions, requires a comprehensive review and therefore, is not included in this literature review.

Currently, there is a lack of comprehensive research on the combined response of GFRP-RCC columns under compression, both in experimental and numerical investigations. The GFRP-RCC columns can be examined by utilising effective numerical techniques, such as the Finite Element Method [79], Bezier Multi-Step Method [80], and Differential Quadrature Method [81]. Elchalakani et al. [53] employed finite element analysis to predict the behaviour of GFRP-reinforced geopolymer and OPC concrete columns under both concentric and eccentric loading, validating their findings with experimental data. The concrete was modelled using C3D8R, which is a reduced integration of 8-noded hexahedral elements. The concrete's elastoplastic material behaviour, as well as the decrease in strength and stiffness after reaching the peak, were simulated using the commonly employed concrete damage plasticity model provided by ABAQUS. Concrete is considered to exhibit linear elastic behaviour in the reversible regime and damaged plasticity behaviour in the irreversible regime. In the case of the GFRP bars and stirrups, their behaviour was considered linear elastic. Various researchers used similar FEM models to validate the load–deflection characteristics of FRP-RCC columns [45, 82].

Additionally, researchers could employ the Bezier-based multi-step method, which is an excellent tool for solving the governing fourth-order complex partial differential equation

Table 6 Design equations available in the literature for axial load carrying capacity of reinforced concrete columns

References	Proposed design equations	Equation no
<i>Steel-RCC columns</i>		
ACI318-08 [67]	$P_d = P_c + P_{bar} = 0.85f_c'(A_g - A_s) + f_y A_s$	1
<i>FRP-RCC columns</i>		
CSA-S806 [69]	$P_d = \alpha_1 f_c'(A_g - A_f), \alpha_1 = 0.85 - 0.0015f_c' \geq 0.67$	2
ACI318-11 [71]	$P_d = 0.85f_c'(A_g - A_f)$	3
Tobbi et al. [73]	$P_d = 0.85f_c'(A_g - A_f) + 0.35f_{fu}A_f$	4
Afifi et al. [74]		
Mohamed et al. [75]	$P_d = 0.85f_c'(A_g - A_f) + 0.002E_{ft}A_f$	5
Hales et al. [76]	$P_d^* = 0.85f_c'(A_g - A_f) + 0.003E_{ft}A_f$	6
Hadi et al. [62]	$P_d^{**} = 0.85f_{cc}(A_c - A_f) + \epsilon_{cc}E_{ft}A_f$	7
Maranan et al. [77]	$P_d = 0.9f_c'(A_g - A_f) + 0.002E_{ft}A_f$	8
Hadhood et al. [78]	$P_d = \beta_1 f_c'(A_g - A_f) + 0.003E_{ft}A_f$ $\beta_1 = 0.85 - 0.0015f_c' \geq 0.67$	9
Hasan et al. [43, 72]	$P_d = 0.85f_c'(A_g - A_f) + \epsilon_{co}E_{ft}A_f$	10

P_d = The proposed maximum axial load-carrying capacity
 A_g = The gross area of the columns
 A_s and A_f = The total cross-sectional area of the longitudinal steel bars and longitudinal FRP bars, respectively
 A_c = The gross area of concrete on the compression side
 f_c' = The compressive strength of the concrete
 f_y = The yield strength of longitudinal steel bars
 f_{fu} = The ultimate tensile strength of longitudinal FRP bars
 f_{cc} = The confined concrete core strength
 E_{ft} = The modulus of elasticity of FRP bars
 ϵ_{cc} = The ultimate concrete strain at second peak stress
 ϵ_{co} = The concrete axial strain at peak stress
 *First peak load
 **Second peak load

(PDE) in linear elastic fracture mechanics (LEFM) problems. This method can be used to solve initial value problems in one dimension and to simultaneously solve Boundary Value Problems (BVPs) in orthogonal directions [80]. The authors propose doing a comprehensive investigation to obtain the most favourable numerical analysis of the load–deflection behaviour of GFRP-RCC columns using multiple numerical methods.

Conclusions

In construction practices, the use of FRP rebar can provide a more cost-effective, improved tensile strength, corrosion-resistant, and non-conductive alternative to steel rebars. This paper presents a comprehensive literature review on the structural behaviour of FRP-RCC columns with a focus on GFRP rebars. There is limited literature concerning investigations into the utilisation of FRP rebar in columns in comparison to their employment in beams and slabs. However, adding to the benefits of using FRP rebar, recent research

investigations have been undertaken to enhance the understanding of the structural properties of FRP-RCC columns for potential utilisation in areas such as coastal regions, buildings susceptible to electromagnetic interference, and environments with high levels of corrosion. The literature review has led to several insightful conclusions.

1. FRP rebar exhibits higher tensile strength and compressive strength in comparison to steel rebar, even though the FRP rebar's compressive strength is approximately 70% of its tensile strength.
2. GFRP-RCC columns outperform steel RCC columns in terms of compressive strength, durability, and ductility under harsh environmental conditions such as corrosion and freeze–thaw cycles. However, under typical standard conditions, GFRP-RCC columns exhibit a slightly lower compressive strength and increased ductility when subjected to normal axial or eccentric loads.
3. The compressive strength of GFRP-RCC columns is within the range of 82–100% and 60–103% of the compressive strength exhibited by conventional

steel-RCC columns in the case of concentrically loaded columns and eccentrically loaded columns, respectively.

4. Irrespective of the loading conditions or concrete type, GFRP-RCC columns exhibit higher ductility than steel-RCC columns. The average percentage increase in ductility for GFRP RCC columns was 17.4%, with a maximum gain of 35.5%. This is due to the different failure mechanisms of steel and FRP rebars under compression and the greater energy absorption capacity of GFRP-RCC columns during post-peak load.
5. For square and circular cross-section GFRP-RCC columns, the percentage strength ratio (f_{FRP}/f_{steel}) decreases as eccentricity increases, whereas for rectangular cross-section GFRP-RCC columns, this ratio increases with increasing eccentricity.
6. For axially loaded GFRP-RCC columns, the average percentage strength ratio based on the type of concrete is ranked in the following order: 97% for HSC, 93% for NSC, 91% for LWSCC, 89% for OPC, and 82% for both RAC and PMC.
7. OPC concrete columns exhibit an increase in percentage strength ratio with rising eccentricity, whereas the percentage strength ratio of HSC, NSC, LWSCC, RAC, and PMC columns reinforced with GFRP longitudinal bars decreases as eccentricity increases.
8. The contribution of GFRP bars accounted for about 50% of the contribution of steel bars in the axial load-carrying capacity of both NSC and HSC specimens.
9. For axially loaded columns, along with an increase in strength capacity, as the P_t increases, the comparative strength ratio of GFRP-RCC columns to steel-RCC columns also rises, making the strength of GFRP-RCC columns almost equal to that of steel-RCC columns.
10. Although increasing the confinement volume of ties increases the strength capacity of columns, it doesn't have much of an impact on the relative strength of axially loaded GFRP-RCC columns compared to steel-RCC columns.
11. A smaller diameter of ties (6 mm) results in a higher relative strength value for GFRP-RCC columns, nearly equivalent to that of steel-RCC columns.
12. In the case of axial loading, the relative ductility index of GFRP-RCC columns compared to steel-RCC columns decreases from 1.5 to 1 as the stirrup percentage volume increases from 0.38 to 1.22% due to the increased ductility of steel-RCC columns.
13. In predicting the design load-bearing capacity of GFRP-RCC columns, it has been found that using the modulus of elasticity to determine the contribution of FRP longitudinal bars and employing concrete com-

pressive strength rather than axial strain in FRP longitudinal bars yields more accurate predictions.

Future scope of research

1. A detailed comparative study of GFRP-RCC columns and steel RCC columns could be beneficial, focusing on parameters such as column shape, slenderness ratio, reinforcement percentages, and concrete type.
2. Future research is needed to evaluate the performance of hybrid steel-FRP composite bars and Large Rupture Strain (LRS)-FRP bars as longitudinal reinforcement in RCC columns, particularly for applications like underwater structures or electromagnetically sensitive environments.
3. Numerical analyses, in conjunction with experimental tests, might be useful for validating results and providing a basis for future parametric studies, given the broader data range that numerical methods can offer.
4. Considering the use of compressive elastic modulus to assess the contribution of FRP bars in FRP-RCC columns, it is suggested that the compressive strength properties of FRP rebars be incorporated in experimental analyses of FRP-RCC columns.
5. Future research can explore the higher ductility observed in FRP rebar-reinforced concrete columns compared to steel-rebar-reinforced columns, with attention to the compressive and tensile behaviour of FRP rebars, their energy absorption capacity after failure, and their composite action during compression testing.
6. More detailed experimental studies are needed on the failure of axially and eccentrically loaded FRP-reinforced concrete columns, focusing on the effects of composite material formulation, fibre orientation, surface treatment modifications, and epoxy characteristics on the bond strength of FRP bars with different diameters. Additionally, the impact of a development length and fibre types (e.g., Carbon Nano Tubes) on bond strength and load-bearing capacity should be studied to find the best configurations for high-stress applications.

Acknowledgements Not applicable.

Declarations

Conflicts of interest On behalf of all authors, the corresponding author states that there is no conflict of interest.

Availability of data and materials The data, materials, and specific figures presented in this review paper have been sourced from the papers discussed within the literature review. Access to these journals and papers has been facilitated through pre-existing subscriptions held by

the National Institute of Technology Meghalaya, India. All efforts have been made to cite sources accurately and attribute them throughout the manuscript.

References

1. Sheikh SA, Uzumeri SM (1980) Strength and ductility of tied concrete columns. *J Struct Div* 106:1079–1102. <https://doi.org/10.1061/JSDEAG.0005416>
2. Wang Y, Huang Y, Fu C (2017) Performance of T-shaped steel reinforced concrete column under high temperature. *Procedia Eng* 210:565–573. <https://doi.org/10.1016/j.proeng.2017.11.115>
3. Firouzi A, Abdolhosseini M, Ayazian R (2020) Service life prediction of corrosion-affected reinforced concrete columns based on time-dependent reliability analysis. *Eng Fail Anal* 117:104944. <https://doi.org/10.1016/j.engfailanal.2020.104944>
4. Qu F, Li W, Dong W et al (2021) Durability deterioration of concrete under marine environment from material to structure: a critical review. *J Build Eng*. <https://doi.org/10.1016/j.jobbe.2020.102074>
5. Hollaway LC (2010) A review of the present and future utilisation of FRP composites in the civil infrastructure with reference to their important in-service properties. *Constr Build Mater* 24:2419–2445. <https://doi.org/10.1016/j.conbuildmat.2010.04.062>
6. James A, Bazarchi E, Chiniforush AA et al (2019) Rebar corrosion detection, protection, and rehabilitation of reinforced concrete structures in coastal environments: a review. *Constr Build Mater* 224:1026–1039. <https://doi.org/10.1016/j.conbuildmat.2019.07.250>
7. Alaoud L, Al-Salloum Y, Abbas H (2021) Experimental investigation for GFRP rebar couplers for reinforced concrete. *J King Saud Univ Eng Sci* 33:104–110. <https://doi.org/10.1016/j.jksues.2020.04.002>
8. Abbood IS, Odaa SA, Hasan KF, Jasim MA (2021) Properties evaluation of fiber reinforced polymers and their constituent materials used in structures—a review. *Mater Today Proc* 43:1003–1008. <https://doi.org/10.1016/j.matpr.2020.07.636>
9. Feng G, Zhu D, Guo S et al (2022) A review on mechanical properties and deterioration mechanisms of FRP bars under severe environmental and loading conditions. *Cem Concr Compos* 134:104758. <https://doi.org/10.1016/j.cemconcomp.2022.104758>
10. Benmokrane B, Rahman H (1998) Durability of fiber-reinforced polymer (FRP) composite for construction. In: *Proceedings of the 1st international conference on durability of composites for construction*
11. Saadatmanesh H, Ehsani MR (1998) Fiber composites in infrastructure
12. Razaqpur AG (2001) ACMB3-III, the third international conference on advanced composite materials in bridges and structures. *Cem Concr Compos* 4:429
13. De Santis S, de Felice G, Napoli A, Realfonzo R (2016) Strengthening of structures with steel reinforced polymers: a state-of-the-art review. *Compos Part B Eng* 104:87–110. <https://doi.org/10.1016/j.compositesb.2016.08.025>
14. Monaldo E, Nerilli F, Vairo G (2019) Basalt-based fiber-reinforced materials and structural applications in civil engineering. *Compos Struct* 214:246–263. <https://doi.org/10.1016/j.compstruct.2019.02.002>
15. Reichenbach S, Preinstorfer P, Hammerl M, Kromoser B (2021) A review on embedded fibre-reinforced polymer reinforcement in structural concrete in Europe. *Constr Build Mater* 307:124946. <https://doi.org/10.1016/j.conbuildmat.2021.124946>
16. Navaratnam S, Selvaranjan K, Jayasooriya D et al (2023) Applications of natural and synthetic fiber reinforced polymer in infrastructure: a suitability assessment. *J Build Eng* 66:105835
17. Luciano R, Sacco E (1998) Damage of masonry panels reinforced by frp sheets. *Int J Solids Struct* 35:1723–1741. [https://doi.org/10.1016/S0020-7683\(97\)00137-6](https://doi.org/10.1016/S0020-7683(97)00137-6)
18. Sherwood EG, Soudki KA (2000) Rehabilitation of corrosion damaged concrete beams with CFRP laminates—a pilot study. *Compos Part B Eng* 31:453–459. [https://doi.org/10.1016/S1359-8368\(99\)00043-8](https://doi.org/10.1016/S1359-8368(99)00043-8)
19. Fan X, Zhang M (2016) Behaviour of inorganic polymer concrete columns reinforced with basalt FRP bars under eccentric compression: an experimental study. *Compos Part B Eng* 104:44–56. <https://doi.org/10.1016/j.compositesb.2016.08.020>
20. Al-Mahmoud F (2017) CFRP reinforcement rods. *Compr Compos Mater II*(3):578–591. <https://doi.org/10.1016/B978-0-12-803581-8.03972-2>
21. Ye YY, Da LS, Feng P, Zeng JJ (2021) Recyclable LRS FRP composites for engineering structures: current status and future opportunities. *Compos Part B Eng*. <https://doi.org/10.1016/j.compositesb.2021.108689>
22. Tighiouart B, Benmokrane B, Gao D (1998) Investigation of bond in concrete member with fibre reinforced polymer (FRP) bars. *Constr Build Mater*. [https://doi.org/10.1016/S0950-0618\(98\)00027-0](https://doi.org/10.1016/S0950-0618(98)00027-0)
23. Sharaky IA, Torres L, Baena M, Vilanova I (2013) Effect of different material and construction details on the bond behaviour of NSM FRP bars in concrete. *Constr Build Mater* 38:890–902. <https://doi.org/10.1016/j.conbuildmat.2012.09.015>
24. Sasmal S, Khatri CP, Ramanjaneyulu K, Srinivas V (2013) Numerical evaluation of bond-slip relations for near-surface mounted carbon fiber bars embedded in concrete. *Constr Build Mater* 40:1097–1109. <https://doi.org/10.1016/j.conbuildmat.2012.11.073>
25. Ibrahim AMA, Wu Z, Fahmy MFM, Kamal D (2016) Experimental study on cyclic response of concrete bridge columns reinforced by steel and basalt FRP reinforcements. *J Compos Constr* 20:1–19. [https://doi.org/10.1061/\(asce\)cc.1943-5614.0000614](https://doi.org/10.1061/(asce)cc.1943-5614.0000614)
26. Ibrahim AMA, Fahmy MFM, Wu Z (2015) Numerical simulation on fracturing bond mechanisms of different basalt FRP bars. *J Japan Soc Civ Eng Ser A2 Appl Mech* 71:I_289-I_298. https://doi.org/10.2208/jscejam.71.i_289
27. Ibrahim AMA, Fahmy MFM, Wu Z (2016) 3D finite element modeling of bond-controlled behavior of steel and basalt FRP-reinforced concrete square bridge columns under lateral loading. *Compos Struct* 143:33–52. <https://doi.org/10.1016/j.compstruct.2016.01.014>
28. Zhao D, Pan J, Zhou Y et al (2020) New types of steel-FRP composite bar with round steel bar inner core: Mechanical properties and bonding performances in concrete. *Constr Build Mater*. <https://doi.org/10.1016/j.conbuildmat.2020.118062>
29. Veljkovic A, Carvelli V, Haffke MM, Pahn M (2017) Concrete cover effect on the bond of GFRP bar and concrete under static loading. *Compos Part B Eng* 124:40–53. <https://doi.org/10.1016/j.compositesb.2017.05.054>
30. Irshidat MR (2020) Improved bond behavior between FRP reinforcing bars and concrete with carbon nanotubes. *Constr Build Mater*. <https://doi.org/10.1016/j.conbuildmat.2020.119562>
31. Taha A, Alnahhal W (2021) Bond durability and service life prediction of BFRP bars to steel FRP under aggressive environmental conditions. *Compos Struct*. <https://doi.org/10.1016/j.compstruct.2021.114034>
32. Shan Z, Liang K, Chen L (2023) Bond behavior of helically wound FRP bars with different surface characteristics in fiber-reinforced

- concrete. *J Build Eng* 65:105504. <https://doi.org/10.1016/j.jobe.2022.105504>
33. Kim YJ, Wang J (2023) Stochastic modeling and design recommendations for bond of UHPC interfaced with steel FRP reinforcing bars. *Constr Build Mater* 367:130297. <https://doi.org/10.1016/j.conbuildmat.2023.130297>
 34. Naser MZ, Hawileh RA, Abdalla JA (2019) Fiber-reinforced polymer composites in strengthening reinforced concrete structures: a critical review. *Eng Struct*. <https://doi.org/10.1016/j.engstruct.2019.109542>
 35. Mugahed Amran YH, Alyousef R, Rashid RSM et al (2018) Properties and applications of FRP in strengthening RC structures: a review. *Structures* 16:208–238. <https://doi.org/10.1016/j.istruc.2018.09.008>
 36. D'Antino T, Andrea Pisani M (2023) Tensile and compressive behavior of thermoset and thermoplastic GFRP bars. *Constr Build Mater* 366:130104. <https://doi.org/10.1016/j.conbuildmat.2022.130104>
 37. AlAjarmeh OS, Manalo AC, Benmokrane B et al (2019) Novel testing and characterisation of GFRP bars in compression. *Constr Build Mater* 225:1112–1126. <https://doi.org/10.1016/j.conbuildmat.2019.07.280>
 38. Khorramian K, Sadeghian P (2021) Material characterisation of GFRP bars in compression using a new test method. *J Test Eval* 49:1037–1052
 39. Deitz DH, Harik IE, Gesund H (2003) Physical properties of glass fiber reinforced polymer rebars in compression. *J Compos Constr* 7:363–366
 40. Chaallal O, Benmokrane B (1993) Physical and mechanical performance of an innovative glass-fiber-reinforced plastic rod for concrete and grouted anchorages. *Can J Civ Eng* 20:254–268
 41. Xiong Z, Lin L, Qiao S et al (2022) Axial performance of seawater sea-sand concrete columns reinforced with basalt fibre-reinforced polymer bars under concentric compressive load. *J Build Eng*. <https://doi.org/10.1016/j.jobe.2021.103828>
 42. Fang S, Li L, Lin L et al (2021) FRP interlocking multi-spiral reinforced square concrete columns: a promising compression application for marine engineering. *Eng Struct* 244:112733. <https://doi.org/10.1016/j.engstruct.2021.112733>
 43. Hasan HA, Karim H, Goaziz HA et al (2023) Performance evaluation of normal- and high-strength concrete column specimens reinforced longitudinally with different ratios of GFRP bars. *Structures* 47:1428–1440. <https://doi.org/10.1016/j.istruc.2022.11.056>
 44. Gamal Gouda M, Mohamed HM, Manalo AC, Benmokrane B (2023) Experimental investigation of concentrically and eccentrically loaded circular hollow concrete columns reinforced with GFRP bars and spirals. *Eng Struct* 277:115442. <https://doi.org/10.1016/j.engstruct.2022.115442>
 45. Raza A, Hechmi El Ouni M, Ali L et al (2022) Structural evaluation of recycled aggregate concrete circular columns having FRP rebars and synthetic fibers. *Eng Struct*. <https://doi.org/10.1016/j.engstruct.2021.113392>
 46. Ali L, El Ouni MH, Raza A (2021) Tests of polypropylene macro synthetic fibers and GFRP reinforced concrete columns subjected to concentric and eccentric loading. *J Build Eng*. <https://doi.org/10.1016/j.jobe.2021.103100>
 47. Bakouregui AS, Mohamed HM, Yahia A, Benmokrane B (2021) Axial load–moment interaction diagram of full-scale circular LWSCC columns reinforced with BFRP and GFRP bars and spirals: experimental and theoretical investigations. *Eng Struct* 242:112538. <https://doi.org/10.1016/j.engstruct.2021.112538>
 48. ElMessalami N, Abed F, El Refai A (2021) Response of concrete columns reinforced with longitudinal and transverse BFRP bars under concentric and eccentric loading. *Compos Struct*. <https://doi.org/10.1016/j.compstruct.2020.113057>
 49. Zhang P, Chen B, Liu Y et al (2021) Experimental study on the axial compression behavior of columns confined by BFRP ties. *Compos Struct* 258:113302. <https://doi.org/10.1016/j.compstruct.2020.113302>
 50. Ge W, Chen K, Guan Z et al (2021) Eccentric compression behaviour of concrete columns reinforced with steel-FRP composite bars. *Eng Struct*. <https://doi.org/10.1016/j.engstruct.2021.112240>
 51. Hassan A, Khairallah F, Mamdouh H, Kamal M (2019) Structural behaviour of self-compacting concrete columns reinforced by steel and glass fibre-reinforced polymer rebars under eccentric loads. *Eng Struct*. <https://doi.org/10.1016/j.engstruct.2019.03.067>
 52. Salah-Eldin A, Mohamed HM, Benmokrane B (2019) Structural performance of high-strength-concrete columns reinforced with GFRP bars and ties subjected to eccentric loads. *Eng Struct* 185:286–300. <https://doi.org/10.1016/j.engstruct.2019.01.143>
 53. Elchalakani M, Karrech A, Dong M et al (2018) Experiments and finite element analysis of GFRP reinforced geopolymer concrete rectangular columns subjected to concentric and eccentric axial loading. *Structures* 14:273–289. <https://doi.org/10.1016/j.istruc.2018.04.001>
 54. Elchalakani M, Ma G (2017) Tests of glass fibre reinforced polymer rectangular concrete columns subjected to concentric and eccentric axial loading. *Eng Struct* 151:93–104. <https://doi.org/10.1016/j.engstruct.2017.08.023>
 55. Barrera AC, Bonet JL, Romero ML, Fernández MA (2012) Ductility of slender reinforced concrete columns under monotonic flexure and constant axial load. *Eng Struct* 40:398–412. <https://doi.org/10.1016/j.engstruct.2012.03.012>
 56. Astm C (1997) 1018: standard test method for flexural toughness and first-crack strength of fiber-reinforced concrete (using beam with third-point loading). Am Soc Test Mater USA
 57. Foster SJ, Attard MM (1997) Experimental tests on eccentrically loaded high strength concrete columns. *Struct J* 94:295–303
 58. Yang J, Wang J, Wang Z (2018) Rectangular high-strength concrete columns confined with carbon fiber-reinforced polymer (CFRP) under eccentric compression loading. *Constr Build Mater* 193:604–622. <https://doi.org/10.1016/j.conbuildmat.2018.10.226>
 59. Hadi MNS (2007) Behaviour of FRP strengthened concrete columns under eccentric compression loading. *Compos Struct* 77:92–96. <https://doi.org/10.1016/j.compstruct.2005.06.007>
 60. Elmesalami N, Abed F, El RA (2021) Concrete columns reinforced with GFRP and BFRP Bars under concentric and eccentric loads: experimental testing and analytical investigation. *J Compos Constr* 25:1–15. [https://doi.org/10.1061/\(asce\)cc.1943-5614.0001115](https://doi.org/10.1061/(asce)cc.1943-5614.0001115)
 61. Pessiki S, Pieroni A (1997) Axial load behavior of large scale spirally reinforced high strength concrete columns. *Struct J* 94:304–314
 62. Hadi MNS, Karim H, Sheikh MN (2016) Experimental Investigations on circular concrete columns reinforced with GFRP bars and helices under different loading conditions. *J Compos Constr* 20:1–12. [https://doi.org/10.1061/\(asce\)cc.1943-5614.0000670](https://doi.org/10.1061/(asce)cc.1943-5614.0000670)
 63. Menegoteo M, Pinto PE (1973) International association for bridge and structural engineering
 64. Anwar N, Qaasim M (2009) Parametric study of reinforced concrete column cross-section for strength and ductility. *Key Eng Mater* 400–402:269–274. <https://doi.org/10.4028/www.scientific.net/kem.400-402.269>
 65. ACI ACI (2019) 318-19 & ACI 318R-19: Building code requirements for structural concrete and commentary. Am Concr Inst Farming Hills, MI, USA
 66. BIS (2000) Plain and reinforced concrete-code of practise. In: IS 456:2000. Bureau of Indian Standards, New Delhi

67. ACI Committee 318 (2008) Building code requirements for structural concrete (ACI 318-08) and commentary. American Concrete Institute
68. Yehia S, Abdelbaky S, Moubarak A, Ibrahim AM (2023) Experimental and analytical codes comparative study for enhanced BFRP R.C. Columns under different types of loading. *Int Rev Civ Eng (IRECE)* 14(3)
69. Cheung MS (2020) CSA standard S806-design and construction of building components with fibre reinforced polymers—a current overview. In: Fourth Canada–Japan workshop on composites. CRC Press, pp 375–384
70. Zadeh HJ, Nanni A (2013) Design of RC columns using glass FRP reinforcement. *J Compos Constr* 17:294–304. [https://doi.org/10.1061/\(asce\)cc.1943-5614.0000354](https://doi.org/10.1061/(asce)cc.1943-5614.0000354)
71. ACI Committee 440.1R-06 (2006) Guide for the design and construction of concrete reinforced with FRP bars. *Am Concr Inst* 44
72. Hasan HA, Sheikh MN, Hadi MNS (2019) Maximum axial load carrying capacity of fibre reinforced-polymer (FRP) bar reinforced concrete columns under axial compression. *Structures* 19:227–233. <https://doi.org/10.1016/j.istruc.2018.12.012>
73. Tobbi H, Farghaly AS, Benmokrane B (2012) Concrete columns reinforced longitudinally and transversally with glass fiber-reinforced polymer bars. *ACI Struct J* 109:551–558. <https://doi.org/10.14359/51683874>
74. Afifi MZ, Mohamed HM, Benmokrane B (2014) Axial capacity of circular concrete columns reinforced with GFRP bars and spirals. *J Compos Constr* 18:1–11. [https://doi.org/10.1061/\(asce\)cc.1943-5614.0000438](https://doi.org/10.1061/(asce)cc.1943-5614.0000438)
75. Mohamed HM, Afifi MZ, Benmokrane B (2014) Performance evaluation of concrete columns reinforced longitudinally with FRP bars and confined with FRP hoops and spirals under axial load. *J Bridg Eng* 19:1–12. [https://doi.org/10.1061/\(asce\)be.1943-5592.0000590](https://doi.org/10.1061/(asce)be.1943-5592.0000590)
76. Hales TA, Pantelides CP, Reaveley LD (2016) Experimental evaluation of slender high-strength concrete columns with GFRP and hybrid reinforcement. *J Compos Constr* 20:1–10. [https://doi.org/10.1061/\(asce\)cc.1943-5614.0000709](https://doi.org/10.1061/(asce)cc.1943-5614.0000709)
77. Maranan GB, Manalo AC, Benmokrane B et al (2016) Behavior of concentrically loaded geopolymer-concrete circular columns reinforced longitudinally and transversely with GFRP bars. *Eng Struct* 117:422–436. <https://doi.org/10.1016/j.engstruct.2016.03.036>
78. Hadhood A, Mohamed HM, Ghrib F, Benmokrane B (2017) Efficiency of glass-fiber reinforced-polymer (GFRP) discrete hoops and bars in concrete columns under combined axial and flexural loads. *Compos Part B Eng* 114:223–236. <https://doi.org/10.1016/j.compositesb.2017.01.063>
79. Ochoa OO, Reddy JN, Ochoa OO, Reddy JN (1992) Finite element analysis of composite laminates. Springer
80. Kabir H, Aghdam MM (2021) A generalised 2D Bézier-based solution for stress analysis of notched epoxy resin plates reinforced with graphene nanoplatelets. *Thin-Walled Struct* 169:108484. <https://doi.org/10.1016/j.tws.2021.108484>
81. Bert CW, Malik M (1997) Differential quadrature: a powerful new technique for analysis of composite structures. *Compos Struct* 39:179–189. [https://doi.org/10.1016/S0263-8223\(97\)00112-8](https://doi.org/10.1016/S0263-8223(97)00112-8)
82. Gholizadeh MR, Safakhah S (2021) Numerical simulation of application effect of FRP on torsional-flexural behavior of RC columns. *Structures* 33:1721–1733. <https://doi.org/10.1016/j.istruc.2021.05.06>

Springer Nature or its licensor (e.g. a society or other partner) holds exclusive rights to this article under a publishing agreement with the author(s) or other rightsholder(s); author self-archiving of the accepted manuscript version of this article is solely governed by the terms of such publishing agreement and applicable law.